

THE PROPAGATION OF UNCERTAINTIES IN STELLAR POPULATION SYNTHESIS MODELING III: MODEL CALIBRATION, COMPARISON, AND EVALUATION

CHARLIE CONROY & JAMES E. GUNN

Department of Astrophysical Sciences, Princeton University, Princeton, NJ 08544, USA

Submitted to the Astrophysical Journal

ABSTRACT

Stellar population synthesis (SPS) provides the link between the stellar and dust content of galaxies and their observed spectral energy distributions. In the present work we perform a comprehensive calibration of our own flexible SPS (FSPS) model against a suite of data. These data include ultraviolet, optical, and near-IR photometry, surface brightness fluctuations, and integrated spectra of star clusters in the Magellanic Clouds (MCs), M87, M31, and the Milky Way (MW), and photometry and spectral indices of both quiescent and post-starburst galaxies at $z \sim 0$. Several public SPS models are intercompared, including the models of Bruzual & Charlot (BC03), Maraston (M05) and FSPS. The relative strengths and weaknesses of these models are evaluated, with the following conclusions: 1) The FSPS and BC03 models compare favorably with MC data at all ages, whereas M05 colors are too red and the age-dependence is incorrect; 2) All models yield similar optical and near-IR colors for old metal-poor systems, and yet they all provide poor fits to the integrated $J-K$ and $V-K$ colors of both MW and M31 star clusters; 3) FSPS is able to fit all of the ultraviolet data because both the post-AGB and horizontal branch evolutionary phases are handled flexibly, while the BC03 and M05 models fail in the far-UV, and both far and near-UV, respectively; 4) All models predict ugr colors too red, D_n4000 strengths too strong and $H\delta_A$ strengths too weak compared to massive red sequence galaxies, under the assumption that such galaxies are composed solely of old metal-rich stars; 5) FSPS and, to a lesser extent, BC03 can reproduce the optical and near-IR colors of post-starburst galaxies, while M05 cannot. Reasons for these discrepancies are explored. The failure at predicting the ugr colors, D_n4000 , and $H\delta_A$ strengths can be explained by some combination of a minority population of metal-poor stars, young stars, blue straggler and/or blue horizontal branch stars, but not by appealing to inadequacies in either theoretical stellar atmospheres or canonical evolutionary phases (e.g., the main sequence turn-off). The different model predictions in the near-IR for intermediate age systems are due to different treatments of the TP-AGB stellar evolutionary phase. We emphasize that due to a lack of calibrating star cluster data in regions of the metallicity-age plane relevant for galaxies, all of these models continue to suffer from serious uncertainties that are difficult to quantify.

Subject headings: stars: evolution — galaxies: stellar content — galaxies: evolution

1. INTRODUCTION

The spectral energy distribution (SED) of a galaxy contains a wealth of information regarding its star formation history, dust content, and chemical abundance pattern. These properties provide essential clues to the physical processes governing the formation and evolution of galaxies from high redshift to the present. It is therefore highly desirable to have a robust method for extracting the physical properties of galaxies from their SEDs.

The process of translating observed SEDs into physical properties is, unfortunately, very challenging because it requires 1) an accurate understanding of all phases of stellar evolution, 2) well-calibrated stellar spectral libraries for converting stellar evolution calculations into measurable fluxes, 3) an initial mass function (IMF), specifying the weight given to each stellar mass, 4) detailed knowledge of the star-dust geometry in conjunction with an appropriate extinction curve; i.e., knowledge of the physical conditions of the interstellar medium (ISM). Each of these requirements depend on chemical composition, further compounding the problem. Combining these ingredients in order to predict the spectrum of a galaxy is known as stellar population synthesis (SPS), and has an extensive history (e.g., Tinsley & Gunn 1976; Tinsley 1980; Bruzual 1983; Renzini & Buzzoni 1986; Buzzoni 1989; Bruzual & Charlot 1993; Worthey 1994; Maraston 1998; Leitherer et al. 1999; Fioc & Rocca-Volmerange 1997;

Vazdekis 1999; Yi et al. 2003; Bruzual & Charlot 2003; Jimenez et al. 2004; Le Borgne et al. 2004; Maraston 2005; Schiavon 2007; Coelho et al. 2007; Conroy et al. 2009a; Mollá et al. 2009; Kotulla et al. 2009).

In the past two decades enormous progress has been made on each of the requirements mentioned above. Yet, substantial uncertainties remain. A non-exhaustive list includes 1) the treatment of the core convective boundary in main sequence stars (i.e., convective core overshooting); 2) metallicity-dependent mass-loss along the red giant branch (RGB) and, relatedly, the morphology of the horizontal branch (HB); 3) the treatment of the thermally-pulsating asymptotic giant branch (TP-AGB) phase; 4) the spectral libraries, especially for M giants, TP-AGB stars, and stars at non-solar metallicities (e.g., Martins & Coelho 2007); 4) blue straggler (BS) stars and their ubiquity (e.g., Preston & Sneden 2000; Li & Han 2008); 5) the effects of binarism, which might be especially relevant for massive star evolution (e.g., Eldridge et al. 2008) and BS stars; 6) the importance of rotation on massive star evolution (e.g., Meynet & Maeder 2000); 7) non-solar abundance ratios, which effect not only the stellar evolution calculations but also the stellar spectra (e.g., Coelho et al. 2007); 8) the unknown dependence of the IMF on ISM properties such as metallicity and pressure. These uncertainties can in many cases dramatically impact the ability to convert observables into physical properties and vice-versa (e.g., Charlot et al. 1996; Charlot 1996;

Yi 2003; Gallart et al. 2005; Maraston et al. 2006; Lee et al. 2007; Conroy et al. 2009a; Muzzin et al. 2009; Conroy et al. 2009b).

Thankfully, there exists a wide array of data capable of constraining SPS models. By far the most common type of object used for comparison is the star cluster¹. The approximately uniform age and metallicity of the stars within star clusters and the lack of internal reddening (except perhaps for very young clusters) affords direct comparison between them and the most basic ingredients in SPS — the stellar evolution calculations and stellar spectral libraries. Comparisons to star clusters are either made in CMD space or in an integrated sense (i.e., the light from all the cluster stars are added together). The former technique provides a sensitive probe of the main-sequence including the turn-off point, sub-giant and red giant branches (e.g., Worthey 1994; Bruzual & Charlot 2003; An et al. 2009), while the latter technique provides a more robust measure of the rarer brightest stars that dominate the integrated light from the cluster. It is the latter method of comparison that is more relevant if the goal of SPS modeling is to understand the integrated light from galaxies. For this reason, the integrated colors, surface brightness fluctuations (SBFs), and spectra of star clusters have been used extensively to compare and calibrate SPS models (e.g., Bruzual & Charlot 2003; González et al. 2004; Maraston 2005; Cohen et al. 2007; Cordier et al. 2007; Pessev et al. 2008; Marigo et al. 2008; Koleva et al. 2008; Lee et al. 2009b).

There are two significant sources of concern when attempting to calibrate SPS models with star cluster data. The first concern is that the brightest stars, which dominate the integrated light, are rare, and thus stochastic effects must be carefully modeled. Recently, this issue has been addressed observationally by stacking clusters in bins of age in order to synthesize ‘superclusters’ that are relatively unaffected by stochastic effects (Pessev et al. 2006; González et al. 2004).

The second concern is less tractable, even in principle, and arises from the fact that the primary sources of star clusters for which ages and metallicities can be reliably estimated are the Milky Way (MW), M31, and the Large and Small Magellanic Clouds (LMC and SMC, respectively). This fact imposes severe restrictions on the region of the age-metallicity parameter space that can be constrained with star cluster data. For example, one of the most important regions of this parameter space for studying galaxies — old and metal rich — contains very few star clusters (except in the bulge of the MW, although high extinction diminishes the utility of star clusters there). In Local Group star clusters, a bin in age contains clusters of a relatively narrow range in metallicity owing to the simple fact that the metallicity of galaxies tends to increase with age.

Because of these issues, entire galaxies are often also used to assess the accuracy of SPS models (e.g., Worthey 1994; Bruzual & Charlot 2003; Maraston et al. 2006; Eminian et al. 2008). Galaxies are not subject to the two concerns mentioned above, but using them to constrain SPS models can be very difficult because 1) galaxies contain stars of a range of ages and metallicities; and 2) starlight in galaxies is attenuated by interstellar dust. Nevertheless, if subsamples of galaxies are carefully constructed with known and regular properties, then galaxies can be used to assess the reliability of SPS models.

The present work seeks to provide a comprehensive comparison between SPS models and observed star clusters and

galaxies. Such a comparison is timely because of an abundance of new, high-quality data, including near-IR photometry and SBFs of star clusters in the LMC and SMC, UV photometry of clusters in M31 and M87, CMDs and integrated spectra of clusters in the MW, and optical and near-IR photometry and spectral indices for large samples of low-redshift galaxies. We will consider not only our own SPS model (Conroy et al. 2009a) but also the commonly used models of Bruzual & Charlot (2003, BC03) and Maraston (2005, M05). Such a detailed comparison between these popular models has not been undertaken until now, and will thus provide a much-needed evaluation of the relative strengths and weaknesses of these models. In addition, the flexible nature of our own model will be exploited to explore the extent to which various uncertain phases of stellar evolution, including thermally-pulsating asymptotic giant branch stars (TP-AGB), blue HB stars, and post-AGB stars, can be constrained by the data. This task is critical if we are to have confidence in the derived physical properties of galaxies, such as stellar masses and star formation rates.

We proceed as follows. §2 contains a detailed description of the star cluster and galaxy data used to constrain the models, which are themselves described in §3. In §4 we present an extensive comparison between models and data. A discussion and summary are provided in §5 and §6, respectively. The zero points of the star cluster UBVRIJK magnitudes are in the Vega system; all other magnitudes are quoted in the AB system (Oke & Gunn 1983). Where necessary, we adopt a flat Λ CDM cosmology with $(\Omega_m, \Omega_\Lambda, h) = (0.26, 0.74, 0.72)$.

2. DATA COMPILATION

This section describes in detail the sources and treatment of data both for star clusters (§2.1) and galaxies (§2.2).

2.1. Star cluster data

The calibration of SPS models against data is essential because of the many uncertain model ingredients, including late stages of stellar evolution and stellar spectral libraries. As mentioned in the introduction, the star cluster is the ideal observational datum for SPS calibration because it is, at least approximately, a coeval set of stars at a single metallicity. In order to provide comprehensive constraints on SPS models, one would like to have data on star clusters spanning a wide range in age, metallicity, and wavelength. Unfortunately, owing to the details of the chemical history of the MW and its satellites, the assembly of such a dataset from nearby galaxies, including our own, is challenging.

In the present work attention is focused on data from the Milky Way (MW), M31, and the Magellanic Clouds (MCs). The first two galaxies are sources primarily of old, metal-poor clusters, while the MCs provide clusters spanning a wider range of ages and metallicities.

Before describing the datasets in detail, it is worth emphasizing those areas of parameter space that are not well-sampled and yet are important for interpreting the integrated light from galaxies. Massive star clusters ($M \gtrsim 10^4 M_\odot$) at solar or super-solar metallicities are not common in the Local Group. Less massive star clusters of such metallicities are more common, but stochastic effects complicates model comparison. The star clusters NGC 6791, NGC 188, and the bulge star clusters NGC 6553 and NGC 6528 are notable exceptions in that they are relatively old and metal-rich. These clusters will be used herein for calibration.

¹ Herein both open and globular clusters will be referred to as star clusters.

2.1.1. The Milky Way

Data on MW star clusters are taken primarily from the globular cluster catalog of Harris (1996). This catalog provides *UBVRI* photometry, [Fe/H] metallicities, and $E(B-V)$ reddening values for 150 clusters. The photometry is corrected for Galactic extinction using the reddening values provided in the catalog in conjunction with a Cardelli et al. (1989) extinction curve. The Harris (1996) catalog is complemented with *JHK* photometry from the Two Micron All Sky Survey (2MASS; Skrutskie et al. 2006) for 106 clusters as compiled by Cohen et al. (2007). For most of the comparisons between models and data the MW sample is restricted to clusters with $E(B-V) < 0.2$ in order to reduce the uncertainties associated with de-reddening. When presenting $V-K$ and $J-K$ colors, all clusters with $E(B-V) < 0.4$ are included since reddening corrections are smaller in the near-IR.

Schiavon et al. (2005) have measured integrated, flux-calibrated, high signal-to-noise spectra of 40 MW star clusters spanning a range of metallicities and HB morphologies. The spectra span the wavelength range $3360 < \lambda < 6430\text{\AA}$ at a FWHM resolution of 3.1\AA and sampling of 1.0\AA . These spectra have been de-reddened using the Cardelli et al. (1989) extinction curve with $E(B-V)$ values tabulated by Schiavon et al. Metallicities are also provided by Schiavon et al. and will be used herein, except for 19 clusters that have updated [Fe/H] measurements from Carretta et al. (2009).

2.1.2. M31

Photometry of star clusters in M31 is available in the Revised Bologna Catalog (RBC v3.5; Galleti et al. 2004). Available photometry includes *UBVRI* from a variety of sources, *JHK* from 2MASS, and new ultraviolet observations from the *Galaxy Evolution Explorer* (*GALEX*; Martin et al. 2005) presented in Rey et al. (2007). Spectroscopic metallicities of a subset of M31 star clusters are taken from Barmby et al. (2000) and Perrett et al. (2002). Galactic $E(B-V)$ reddening estimates are derived from Schlegel et al. (1998) via the utilities in the `kcorrect v4.1.4` software package (Blanton & Roweis 2007). Photometry is corrected for Galactic extinction via $E(B-V)$ and the extinction curve of Cardelli et al. (1989). In addition to Galactic reddening, the colors of M31 star clusters will also be reddened by dust within M31. Unfortunately it is not straightforward to make such a correction, and therefore no additional correction will be applied. In later sections attention will be focused on the near-IR colors of M31 clusters, where dust corrections should be small.

The RBC contains a number of quality flags. Clusters are selected to be definite globular clusters (classification flag =1), with a definite confirmation (confirmation flag =1), and to not be in the young cluster catalog of Fusi Pecci et al. (2005). This sample is further restricted to clusters with $E(B-V) < 0.2$ to reduce the uncertainties associated with Galactic reddening.

The final cluster catalog, which includes the aforementioned quality cuts and metallicity measurements, contains 22 clusters, 20 of which include *GALEX NUV* photometry, and 12 of which include *GALEX FUV* photometry.

2.1.3. The Magellanic Clouds

Data on star clusters in the MCs come principally from two sources. Pessev et al. (2006) presented a carefully constructed catalog of 2MASS *JHK* photometry for a sample of 75 star

clusters. In Pessev et al. (2008) this near-IR photometry is combined with *BV* photometry from the literature. These authors construct a ‘test sample’ of star clusters where high quality data are available to estimate main sequence turn-off ages from CMDs and metallicities from either the CMDs or individual stellar spectroscopy. These high-quality data are then binned by age to produce average colors and metallicities as a function of cluster age.

In the youngest age bin a less direct method is used for determining cluster ages in the Pessev et al. (2008) sample. The ‘S-parameter’, introduced by Elson & Fall (1985), provides a simple empirical relation between cluster age and a combination of integrated $U-B$ and $B-V$ colors. High quality age estimates from HST observations from Kerber et al. (2007) were used by Pessev et al. (2008) to update the S-parameter-age calibration in order to provide age estimates for the youngest clusters in their sample. The Pessev et al. calibration is substantially different from the commonly used relation of Girardi et al. (1995). It is important to keep in mind that since ages are based on CMD fitting, they will depend on the stellar evolution calculations used to convert main sequence turn-off points into ages. In particular, the treatment of convective overshooting has a strong impact on the age-main sequence turn-off point relation for young and intermediate ages ($t \lesssim 2 \times 10^9$ yrs). This sensitivity arises because overshooting increases the amount of fuel available for core hydrogen burning. We will return to these issues when these data are compared to models.

The second significant source of data on MC star clusters comes from González et al. (2004). These authors analyze 2MASS data to produce not only integrated near-IR colors but also surface brightness fluctuations in the 2MASS *JHK* filters. Clusters are stacked according to the classification system devised by Searle et al. (1980, SWB), which closely tracks the S-parameter described above. The relation between SWB type, age and metallicity is adopted from Cohen (1982). We have independently verified that these ages agree with the ages inferred from the S-parameter calibration discussed in Pessev et al. (2008). This sample has been augmented with $V-I$ colors (González-Lópezlira et al. 2005), where I magnitudes are from the DENIS survey (Epchtein et al. 1997) and V magnitudes are taken from van den Bergh (1981). We point out that the Pessev et al. and Gonzalez et al. samples are not disjoint. Comparison of these two catalogs will provide a valuable cross-check on the reliability of the data.

The novel feature of these two datasets is that the cluster data have been stacked in bins of age in order to reduce stochastic effects. A number of authors have discussed the importance of stochastic effects arising from small numbers of very bright stars (Lançon & Mouhcine 2000; Bruzual A. 2002; Cerviño & Luridiana 2004; Bruzual & Charlot 2003). Both Lançon & Mouhcine (2000) and Cerviño & Luridiana (2004) provide limits on the minimum cluster mass that should be satisfied so that stochastic fluctuations in integrated colors are minimized. Pessev et al. (2008) demonstrate that the masses of their stacked clusters easily satisfy both constraints, ensuring that their stacked results can be robustly compared to SPS models. The masses of the stacked clusters in the González et al. (2004) sample are comparable to those in Pessev et al. (2008), and so their results should also be relatively unaffected by stochastic effects.

Finally, we include for completeness the $V-K$ and $J-K$ colors of LMC clusters from Persson et al. (1983), which have

been used in many comparisons between observations and SPS models. These J and K magnitudes are converted from the California Institute of Technology (CIT) photometric system to the 2MASS system using the transformations provided by Carpenter (2001). Ages for these clusters were assigned based on the S -parameter calibration of Pessev et al. (2008).

Pessev et al. (2006) presented a detailed comparison between their near-IR colors and those of Persson et al. (1983), in some cases noting substantial differences in the sense that colors from Persson et al. were redder than the colors from Pessev et al. They attributed this difference to the fact that Persson et al. centered their photometry on the brightest part of the cluster in order to maximize the measured flux, while Pessev et al. center their apertures using a Gaussian smoothing technique. In some cases the Persson et al. centroids are significantly offset from the true dynamical center of the cluster because of off-center IR-bright sources within the cluster. For this reason, in addition to the fact that the data are stacked to reduce stochastic effects, the results of Pessev et al. should be preferred to the older results of Persson et al. We will return to this issue in §4.

2.2. Galaxy data

2.2.1. The utility of galaxies

For the reasons mentioned in the previous section, star clusters are the ideal observational data to calibrate SPS models. There are however at least two reasons why it is useful to also consider SPS constraints from galaxies: 1) galaxies tend to be of higher metallicity than old star clusters, and so SPS model predictions for old $\sim Z_{\odot}$ populations can be assessed with galaxies composed of old stars; 2) galaxies contain many more stars than star clusters, and so stochastic effects are never a source of concern when comparing models to galaxy data.

These two benefits of using galaxies to calibrate SPS models are exploited herein by considering two classes of galaxies. The first class consists of bright red sequence, ‘quiescent’ galaxies, which contain old metal-rich stars, and will therefore be useful for calibrating old metal-rich SPS model predictions. The second class are called ‘K+A’, or ‘post-starburst’ galaxies, as their spectra are dominated by a mixture of A and K type stars and show no signs of ongoing star formation (e.g., Dressler & Gunn 1983; Goto et al. 2003). Such galaxies are presumed to have had their star formation abruptly truncated. The presence of A stars in their spectra indicates that the galaxy contains a significant population of $\lesssim 1$ Gyr old stars (e.g., Leonardi & Rose 1996). These galaxies will provide valuable constraints on the importance of TP-AGB stars, as the prominence of this stellar phase peaks for ages $\approx 1-2$ Gyr (Maraston 2005; Conroy et al. 2009a). Since stars spend a small amount of time in this phase, observational constraints from star clusters can be difficult to interpret because of stochastic variations. As mentioned above, a stacking technique is employed when comparing to star clusters so that stochastic effects are minimized. Nonetheless, it will be useful to derive independent constraints from galaxies where stochastic effects are known to be negligible.

As mentioned in the introduction, the use of galaxies to assess the accuracy of SPS models is complicated by at least two effects: the attenuation of starlight by dust and the fact that galaxies contain stars of a range of ages and metallicities. These complications are addressed where relevant in §4.

2.2.2. Data sources

The source of all galaxy positions, optical photometry, and redshifts is the Sloan Digital Sky Survey (SDSS; York et al. 2000), as made available through the hybrid NYU Value Added Galaxy Catalog² (VAGC; Blanton et al. 2005). The SDSS photometry is k -corrected and corrected for Galactic extinction via the `kcorrect v4.1.4` software package (Blanton & Roweis 2007). The photometry is k -corrected to $z = 0.1$ – the median redshift of the sample – in order to minimize the magnitude of the k -correction. Spectroscopic indices are provided by the MPA/JHU database³.

Near-IR photometry in $YJHK$ filters is provided by the UKIRT Infrared Deep Sky Survey⁴ (UKIDSS). The UKIDSS project is defined in Lawrence et al. (2007). UKIDSS uses the UKIRT Wide Field Camera (WFCAM; Casali et al. 2007). The photometric system is described in Hewett et al. (2006), and the calibration is described in Hodgkin et al. (2009). The pipeline processing and science archive are described in Irwin et al (2009, in prep) and Hambly et al. (2008). We make use of Data Release 3, which is publicly available. UKIDSS photometry is matched to the SDSS with a search radius of $5''$. Petrosian magnitudes are used for the UKIDSS photometry. We do not consider colors that are combinations of SDSS and UKIDSS photometry, so it is not essential that the photometric apertures be precisely matched.

The UKIDSS survey goes much deeper than 2MASS, and is therefore more desirable. For example, typical 2MASS photometric errors for galaxies at $z \sim 0.1$ are 0.2 mags, compared to ~ 0.01 for UKIDSS photometry. Galactic extinction is corrected using $E(B-V)$ reddening estimates (Schlegel et al. 1998) in conjunction with a Cardelli et al. (1989) extinction curve. K -corrections for the UKIDSS photometry are estimated from the `kcorrect v4.1.4` software package using the 2MASS JHK filters since those, and not UKIDSS filters, are available in the code. The filter transmission curves for 2MASS and UKIDSS are very similar and so this approximation is justified.

Three galaxy samples are considered. The first are K+A galaxies as identified by Quintero et al. (2004). This sample contains 1194 galaxies. Of these, only 186 have UKIDSS photometry. When considering near-IR colors of the K+A sample we use only these 186 galaxies, while when SDSS colors are considered we use the full sample.

The second sample consists of bright red sequence (‘quiescent’) galaxies. This sample is defined by $M_r^{0.1} < -20.5$, where the superscript indicates that the magnitude has been k -corrected to $z = 0.1$, and

$$(g-r)^{0.1} > -0.03(M_r^{0.1} + 23.0) + 0.94, \quad (1)$$

which divides galaxies by the valley visible in the color-magnitude diagram and effectively isolates red sequence galaxies. Applying these cuts and requiring that galaxies have both SDSS and UKIDSS photometry results in a sample of 5340 galaxies at $0.08 < z < 0.12$.

The third sample is derived from the spectroscopic indices catalog. Galaxies are selected with $0.05 < z < 0.1$ and with a median spectroscopic signal-to-noise of $S/N > 25$. From this catalog two classes of galaxies are defined: those with velocity dispersions measured from the stellar continuum of

² <http://sdss.physics.nyu.edu/vagc/>

³ <http://www.mpa-garching.mpg.de/SDSS/>

⁴ <http://www.ukidss.org/>

$100 < \sigma < 200 \text{ km s}^{-1}$ and those with $\sigma > 200 \text{ km s}^{-1}$. These samples contain 13214 and 6774 galaxies, respectively.

3. SPS MODEL CONSTRUCTION

3.1. Flexible SPS

3.1.1. Theoretical isochrones

SPS model construction closely follows that of Conroy et al. (2009a), to which the reader is referred for details. In brief, this SPS code (referred to below as FSPS, for ‘flexible’ SPS) combines stellar evolution calculations with stellar spectral libraries to produce simple stellar populations (SSPs), which describe the evolution in time of the spectrum of a mono-metallic, coeval set of stars. The initial stellar mass function (IMF) specifies the weights given to stars of various masses. The IMF of Kroupa (2001) is adopted throughout. FSPS also contains a number of phenomenological dust attenuation prescriptions and produces spectra for composite stellar populations. Our SPS code is open-source and publicly available⁵.

The novel feature of this SPS model is that the essential aspects of SPS are integrated in a flexible way so that the user may choose, for example, their preferred set of isochrones and stellar spectral libraries. In addition, the user may alter the weights given to and physical parameters of various advanced stages of stellar evolution (see below), and may specify the IMF of their choosing. The details of these various model choices are now described.

We make use of both the Padova⁶ (Girardi et al. 2000; Marigo & Girardi 2007; Marigo et al. 2008) and BaSTI⁷ (Pietrinferni et al. 2004; Cordier et al. 2007) stellar evolution calculations, both in the versions available as of November 2009. These two groups follow stellar evolution from the main sequence through the thermally-pulsating asymptotic giant branch (TP-AGB) phase, although the treatment of the TP-AGB phase is very different between the two groups.

The Padova calculations exist for metallicities in the range $2 \times 10^{-4} < Z < 0.030$, for ages $10^{6.6} < t < 10^{10.2}$ yrs, and for initial masses $0.15 \leq M \leq 67 M_{\odot}$. BaSTI outputs cover a somewhat narrow range in ages, $10^{7.5} < t < 10^{10.2}$ yrs, and initial masses $0.5 \leq M \leq 10.0 M_{\odot}$ but include higher metallicities: $3 \times 10^{-4} < Z < 0.040$. The BaSTI database provides models for both solar-scaled and α -enhanced chemical compositions, for two assumptions regarding convective core overshooting, and for two stellar mass-loss rates. We use the solar-scaled, no overshooting, and $\eta = 0.4$ mass-loss rate parameter model. For both lower and higher masses the Padova calculations are stitched onto the BaSTI grid. The Padova and BaSTI models are compared in Figure 1. In this figure isochrones are compared at several ages and metallicities, and in addition the location of the TP-AGB onset is shown.

In order to follow stellar evolution from the end of the TP-AGB phase through the post-AGB phase, the above evolutionary tracks have been supplemented with the post-AGB models of Vassiliadis & Wood (1994). The contribution of post-AGB stars to the integrated SED is highly uncertain for a number of reasons, including a lack of calibrating observations and the unknown duration of heavy enshrouding as post-AGB stars leave their M giant phase. Recent observations of M32 have found that post-AGB stars are much less

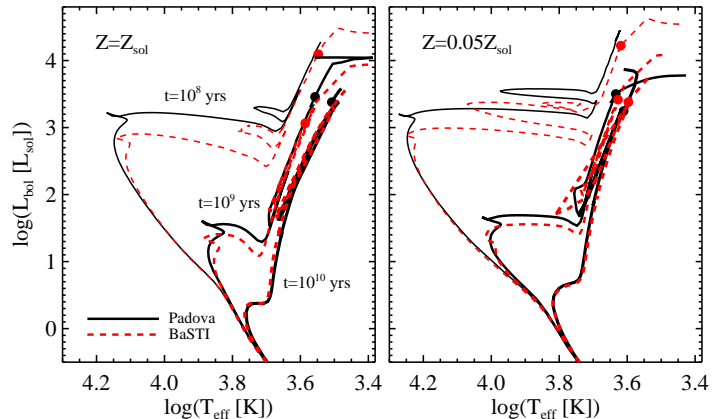


FIG. 1.— Theoretical HR diagram comparing the BaSTI and Padova evolutionary calculations at several ages and metallicities. Isochrones are plotted from the main sequence through the TP-AGB phase. The onset of the TP-AGB phase is marked by solid symbols along each isochrone. The 10^{10} yr solar metallicity BaSTI isochrone and the 10^8 yr Padova isochrones do not contain TP-AGB stars. The difference between the models at young ages is due to the different treatments of convection in the two models (i.e., the handling of convective core overshooting).

frequent than standard models predict (Brown et al. 2008). Nonetheless, the inclusion of post-AGB tracks may be important for the interpretation of the ultraviolet spectra of old systems (e.g., Greggio & Renzini 1990).

The FSPS code contains a number of parameters that control the weights given to various uncertain phases of stellar evolution. For example, the bolometric luminosity and effective temperature of TP-AGB stars can be arbitrarily modified. These modifications are applied as overall shifts in $\log(L_{\text{bol}})$ and $\log(T_{\text{eff}})$ for the entire TP-AGB phase, and are parameterized by the variables Δ_L and Δ_T (see discussion in Conroy et al. 2009a). In addition, an extended blue HB can be included⁸, as can a population of BS stars. A blue HB population is parameterized as the fraction, f_{BHB} of HB stars that are in a blue/extended component. Such a flexible treatment is motivated by the great variety of observed HB morphologies in MW clusters, even at a given metallicity (Piotto et al. 2002). These stars are uniformly populated from the red clump to $\log(T_{\text{eff}}/K) = 4.2$. BS stars are uniformly populated from one half magnitude above the main sequence turn-off to two and a half magnitudes brighter than the turn-off, along the zero-age main sequence (Xin & Deng 2005). The weight given to BS stars is specified as the number of BS stars per unit HB star, S_{BS} . The weight given to the post-AGB phase can also be arbitrarily modified. The effect of these uncertain aspects of stellar evolution will be investigated in later sections.

3.1.2. Spectral libraries

Stellar spectral libraries are required to convert the outputs of stellar evolution calculations — surface gravities, g , effective temperatures, T_{eff} , and metallicities, Z , — into observable spectral energy distributions. Two spectral libraries are considered herein. The first is the empirically-calibrated theoretical BaSeL3.1 library (Lejeune et al. 1997, 1998; Westera et al. 2002), supplemented with empirical, average

⁵ www.astro.princeton.edu/~conroy/SPS/

⁶ <http://stev.oapd.inaf.it/cgi-bin/cmd>

⁷ <http://www.oa-teramo.inaf.it/BASTI>

⁸ When we consider blue/extended HB populations we do not add new stars but rather move stars from the red clump HB to the blue component.

TP–AGB spectra from the library of Lançon & Mouhcine (2002). The BaSeL library was constructed from the model atmospheres of Kurucz (1995, private communication to R. Buser), Fluks et al. (1994), Bessell et al. (1989, 1991), and Allard & Hauschildt (1995). In the TP–AGB library, spectra are binned both by near–IR color and by whether the star is carbon–rich or oxygen–rich. Stars hotter than 50,000K are assumed to be pure blackbodies. This combined library covers the full wavelength range (ultraviolet through infrared) at a sampling of 10Å in the ultraviolet and 20Å in the optical.

The second spectral library considered herein is derived from the empirical Miles library (Sánchez-Blázquez et al. 2006). This atlas contains spectra of ≈ 1000 stars covering the wavelength range $3600 < \lambda < 7500\text{Å}$ at a sampling of 0.9Å per pixel (FWHM $\approx 2.3\text{Å}$). Derived stellar parameters are presented in Cenarro et al. (2007). Integrating empirical libraries into SPS models is a non–trivial task because the coverage in the stellar parameters g , T_{eff} , and Z is very inhomogeneous. In fact many regions of this parameter space are not covered by empirical libraries at all, especially at sub–solar and super–solar metallicities and for spectral types earlier than A. An additional problem with the Miles library is that the spectra have been arbitrarily normalized to unity at 5350Å. This is particularly problematic because the wavelength range is not broad enough to compare the integral of the flux to the bolometric luminosity for a star with a given g , T_{eff} , and Z . Therefore, an additional library must be used to provide the absolute flux scale. The BaSeL library is used for this purpose. The BaSeL library is also used to provide the relative trends of spectra with stellar parameters for regions of parameter space where the relative trends cannot be self–consistently determined from Miles. The Miles library is binned and, when necessary, linearly interpolated onto the Kurucz/BaSeL $\log(g)$ – $\log(T_{\text{eff}})$ grid. This interpolated library is then interfaced with FSPS in a manner identical to the BaSeL library. Five metallicity bins are defined so that roughly similar numbers of stars occupy each bin. The bin boundaries are: $\log(Z/Z_{\odot}) = [-2.0, -1.0, -0.5, -0.15, 0.15, 0.75]$. The resulting average metallicities within these bins are $\log(Z/Z_{\odot}) = [-1.4, -0.7, -0.3, 0.0, 0.2]$.

At metallicities less than solar, the Miles library stars are α –enhanced (Milone et al. 2009). At $[\text{Fe}/\text{H}] < -1$ the library is on average enhanced in Mg by +0.4 dex. This will be relevant in our comparison to the spectra of MW star clusters in later sections.

There are several important caveats to these libraries that the reader should keep in mind. In the empirical TP–AGB library, the metallicities of the stars are *unknown*. The authors advocate assuming that they are all solar metallicity since a significant fraction are located in the solar neighborhood (although many are also located in the MCs). In order to use the library at non–solar metallicities, the authors suggest the use of the theoretical metallicity–dependent color–temperature relations in Bessell et al. (1991) in order to convert the observed I – K colors into temperatures at other metallicities.

Westera et al. (2002) found that the original theoretical atmosphere calculations used in the BaSeL library could not simultaneously match observed $UBVRIJHKL$ color–temperature relations for individual stars and CMDs of globular clusters. The reason for this was thought to be inadequacies in the stellar evolution calculations used in the CMD comparisons. Because of this problem, Westera et al. (2002)

presented two normalizations of the BaSeL library, one which matched the color–temperature relations, and the other which matched the globular cluster data. These two normalizations are referred to as the ‘WLBC’ and PADOVA2000’ libraries, since the Padova evolutionary calculations were used in the globular cluster comparisons. The ‘WLBC’ normalization will be used herein because this calibration is not tied to any particular isochrone set.

In summary, we have in hand a flexible SPS model from which we can choose two sets of isochrones (Padova or BaSTI) and two sets of spectral libraries (BaSeL or Miles). In addition, there are a number of free parameters characterizing various uncertain aspects of advanced stages of stellar evolution. These various options will be exploited in later sections.

3.1.3. Modifications to the Padova isochrones

For the Padova isochrones, the TP–AGB phase has been modified in order to generate acceptable agreement with the data. Specifically, the TP–AGB phase has been calibrated against both MC star clusters and post–starburst galaxies (§4.2 and §4.6, respectively). These calibrations result in an adjustment of the TP–AGB parameters Δ_L and Δ_T (quantifying overall shifts in $\log(L_{\text{bol}})$ and $\log(T_{\text{eff}})$; see §3.1) as follows:

$$\Delta_L = \begin{cases} -1.0 + (t - 8.0)/1.5, & 8 < t < 9.1 \\ -\max\{\min\{0.4, -\log(Z/Z_{\odot})\}, 0.2\}, & t > 9.1, \end{cases} \quad (2)$$

$$\Delta_T = \begin{cases} \begin{cases} +0.1, & \log(Z/Z_{\odot}) < -0.25 \\ 0.0, & \text{otherwise} \end{cases} & 8 < t < 9.1 \\ +0.1 - \min\{(t - 9.1)/1.5, 0.2\}, & t > 9.1, \end{cases} \quad (3)$$

where t is the age of the population measured in $\log(\text{yrs})$. We emphasize that the values of Δ_L and Δ_T chosen to fit the data are *not unique*, and that, unless explicitly stated in the above definitions, they are independent of metallicity. Throughout, reference to the ‘modified Padova model’ refers to these modifications.

3.2. Additional SPS models

We now describe the salient aspects of the BC03 and M05 SPS models.

The BC03 model utilizes the Padova isochrones circa 1994 (Alongi et al. 1993; Bressan et al. 1993; Fagotto et al. 1994), supplemented with the Vassiliadis & Wood (1993) models for TP–AGB stars and the Vassiliadis & Wood (1994) models for post–AGB stars. BC03 use the models of Groenewegen & de Jong (1993) to differentiate between carbon–rich and oxygen–rich TP–AGB stars. There are no blue/extended HB stars in the BC03 models. Their models are constructed with both the theoretical BaSeL library (described in the previous section) and the empirical STELIB library (Le Borgne et al. 2003). Spectra for carbon stars are taken from model atmosphere calculations (Höfner et al. 2000).

The empirical STELIB library contains optical spectra for 249 stars at a resolving power of $R \approx 2000$ (FWHM $\sim 3\text{Å}$). The effective temperatures in the STELIB library are not reliable and so BC03 adopt the color–temperature scale from the BaSeL library in order to relate the stellar evolutionary outputs to the empirical library. There are very few stars at non–solar metallicities and so the reliability of models constructed with this library at non–solar metallicities is questionable. Indeed, Koleva et al. (2008) compared several different SPS models and found that the BC03 model constructed

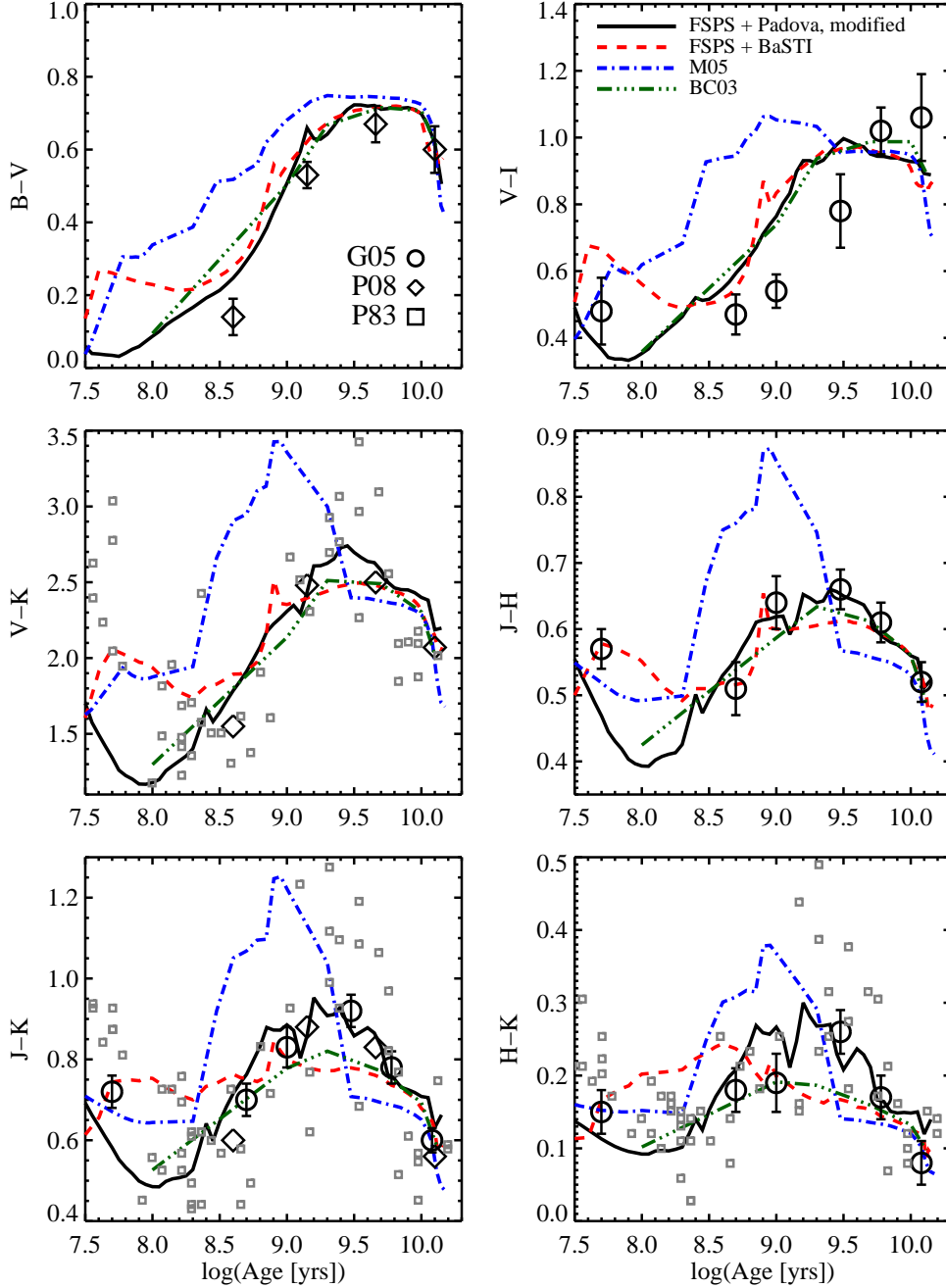


FIG. 2.— SSP colors as a function of age, comparing a variety of SPS models to observations. Data are derived from MC star clusters. The model SSPs include the predictions from M05 (*dot-dashed lines*), BC03 (*dot-dot-dot-dashed lines*) and two models derived from the present work. Using our FSPS code, a model was constructed using the BaSTI (*dashed lines*) and the modified Padova stellar evolution calculations (*solid lines*). The MC data are from Persson et al. (1983, P83), González-Lópezlira et al. (2005, G05) and Pessev et al. (2008, P08). For the latter two data sets, each data point represents an average over many observed star clusters within each age bin. The Persson data is believed to be less reliable for reasons described in the text. The average metallicity of the data decreases as the age increases, from $\log(Z/Z_{\odot}) = -0.3$ at $\log(t)=7.5$ years to $\log(Z/Z_{\odot}) = -1.5$ at $\log(t)=10.0$ years. The model predictions reflect this change in average metallicity with age.

with STELIB produces unreliable results at non-solar metallicities.

We make use of the BC03 model that was constructed with the STELIB library for the optical spectra. For both ultraviolet and near-IR predictions, the STELIB library has been extended with the BaSeL library.

The M05 model is built from the following ingredients. Stellar evolution calculations through the main sequence turnoff are adopted from Cassisi et al. (Cassisi et al. 1997, 2000). The fuel consumption theorem (Renzini & Buzzoni 1986; Maraston 1998) is then used to incorporate advanced stages of stellar evolution through the TP-AGB phase. The

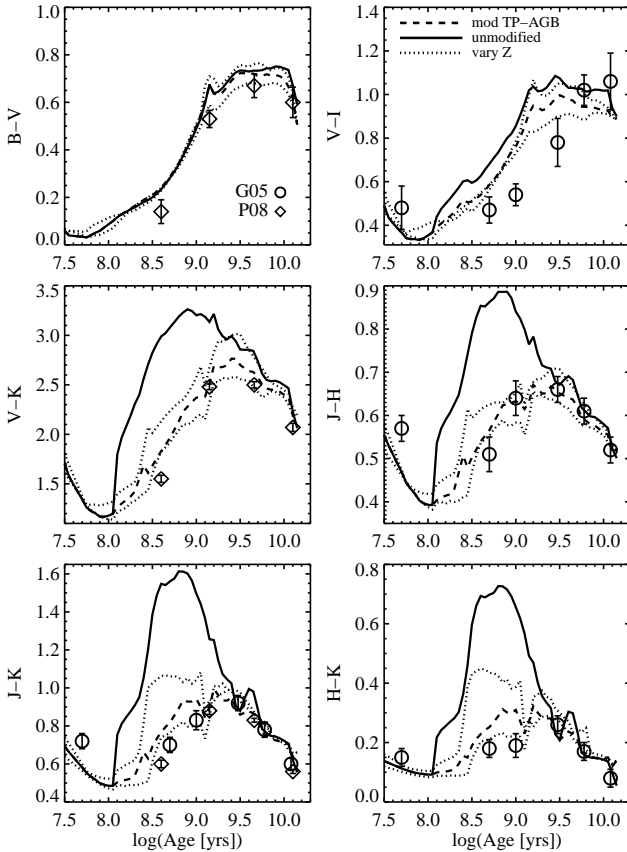


FIG. 3.— SSP colors as a function of age, demonstrating the sensitivity to the TP-AGB phase. The Padova stellar evolution calculations are used for the model predictions. The modified model shown in Figure 2 (dashed lines) is compared to the unmodified Padova calculations (solid lines). Dotted lines correspond to a ± 0.2 dex variation in metallicity about the modified model. The data are from star clusters in the MCs, as in Figure 2. Notice the different y-axis ranges in the bottom panels compared to Figure 2.

evolutionary calculations are converted to observables with the theoretical BaSeL spectral library for all stars except TP-AGB stars. For these stars the empirical library of Lançon & Mouhcine (2002) is used (this is the same library used in our FSPS code).

Model magnitudes and spectral indices⁹ are computed self-consistently from the model spectra. Comparisons between models in later sections are therefore not plagued by potentially different filter transmission curves or index definitions.

4. SPS MODEL CALIBRATION & COMPARISON

4.1. Overview

We now turn to a comparison between observations and SPS models. In §4.2–4.3 we focus on star clusters, both in the MCs, where constraints are strong for intermediate age, sub-solar metallicities, and in the MW and M31, where constraints are strong for old metal-poor systems. We then turn to galaxies in §4.4–4.6. Two types of galaxies will be considered: massive red sequence galaxies and post-starburst galaxies. The former class will provide a qualitative assessment of

⁹ Spectroscopic indices are defined by the wavelength intervals specified in the MPA/JHU database. The intervals are similar to the classic Lick/IDS system (Worthey et al. 1994), although no attempt has been made to ensure that our indices are on the Lick system scale.

the accuracy the SPS models in the solar to super-solar metallicity, old age regime. The post-starburst galaxies will provide an assessment of the models in the approximately solar metallicity, intermediate age regime. As discussed in previous sections, it is challenging to use galaxies to assess the accuracy of SPS models because galaxies are composed of stars with a range of ages and metallicities and dust reddening can be important. These complications are discussed extensively in §4.4–4.6.

4.2. Constraints from the Magellanic Clouds

4.2.1. Colors

Figure 2 shows the colors of MC star clusters as a function of cluster age. As discussed in §2.1.3, individual clusters are binned in age to produce ‘superclusters’ that are relatively immune to stochastic fluctuations (Pessev et al. 2008; González-Lópezlira et al. 2005). The data from Persson et al. (1983) are also included, and have not been binned in age. These data are of inferior quality (see §2.1.3) and are only included for comparison because this data is frequently used to constrain SPS models (e.g., Maraston 2005).

A variety of SPS models are compared to the MC star cluster data in Figure 2. From our FSPS code we have generated SSP color evolution for both the Padova and BaSTI isochrones. In this figure we make use of the modified Padova isochrones (see §3.1.3). The models of BC03 and M05 are also included. All model predictions reflect the fact that the average metallicity of the data varies with age. That is, we have interpolated model predictions so that they vary with metallicity in as in the data, where the age–metallicity relation in the MC data is $\log(t/\text{yrs}) = (7.0, 7.7, 8.7, 9.0, 9.5, 9.8, 10.1)$, $\log(Z/Z_{\odot}) = (-0.28, -0.28, -0.28, -0.28, -0.38, -0.68, -1.5)$ (Pessev et al. 2008; González-Lópezlira et al. 2005).

The M05 models are significantly redder than the data at intermediate ages, owing to the different TP-AGB treatment in M05 (see also Pessev et al. 2008, who reach similar conclusions). The M05 colors also have an age-dependence that does not agree with the data. The MC cluster ages were estimated via CMD fitting using isochrones that include convective overshooting (Kerber et al. 2007; Pessev et al. 2008), whereas the M05 models do not include overshooting, and so one might expect some mismatch in age between the M05 models and data. However, the differences induced by the treatment of overshooting on the MC ages is $\lesssim 0.2$ dex at ages $10^8 \lesssim t \lesssim 10^9$ yrs, whereas the discrepancy in the age-dependence between M05 and the data is > 0.5 dex in age. We therefore regard most of this discrepancy as a shortcoming of the M05 model, with only a fraction being due to different definitions of cluster age.

The Persson et al. data are substantially redder than the newer datasets from Pessev et al. and Gonzalez-Lopezlira et al. As discussed in Pessev et al. (2006), this is probably due to the fact that the Persson photometry was probably centered on the brightest star in the cluster, which are often carbon stars, and in any case are very red, and so the photometry will be biased red. The difference between Persson’s data and the 2MASS-based data highlights the care that must be taken to construct datasets that can be meaningfully used for SPS model calibration.

The M05 models were calibrated against color-color plots of MC star clusters using the Persson et al. data and very wide age bins. Stochastic effects will tend to smear star clusters along an underlying color-color relation because if a cluster is

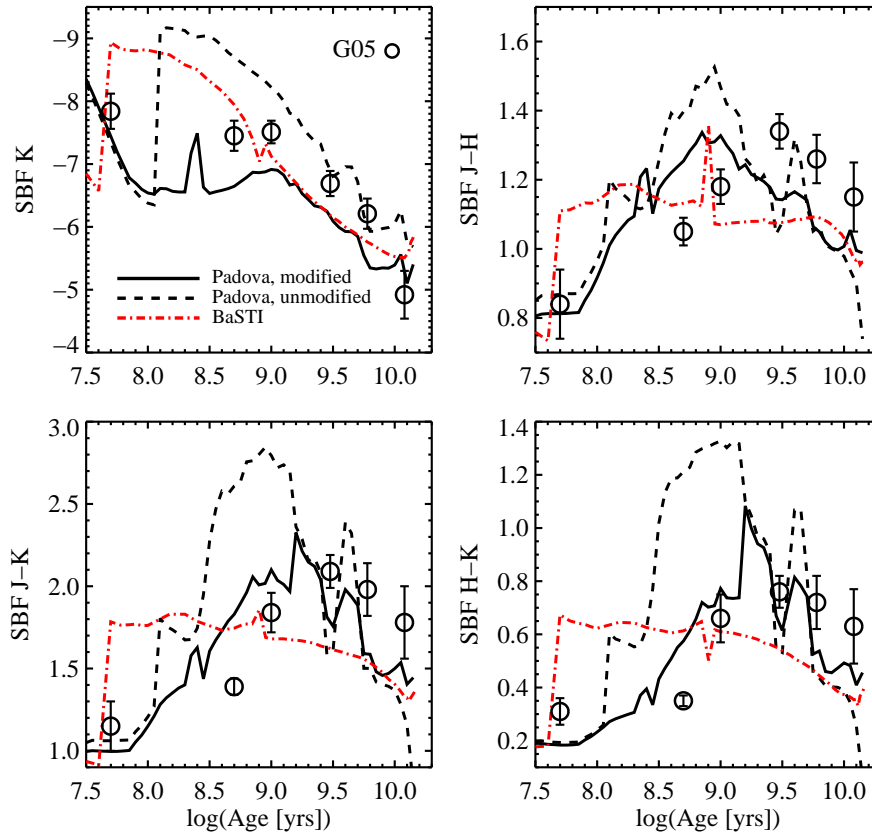


FIG. 4.— SSP surface brightness fluctuation (SBF) magnitudes and colors as a function of age. Models are compared to data from star clusters in the MCs (González-Lópezlira et al. 2005, G05; *symbols*). The models are based on our FSPS code using the Padova and BaSTI isochrones. For the Padova isochrones, predictions are included both for the unmodified and modified isochrones.

scattered redder in one color, it will be redder in another color as well. The M05 model calibration is therefore sensitive to stochastic effects, and is in addition plagued by the systematics in the Persson data. Moreover, the wide age bins used in M05 explains why the discrepancies in age seen for the M05 model in Figure 2 were not seen in their own calibrations.

The BC03 model and BaSTI isochrones both fare well except for $H-K$ and $J-K$ colors at intermediate ages ($\log(t/\text{yrs}) \approx 9.5$), for which models are too blue by ≈ 0.1 mags compared to the data. This disagreement is probably due to the simplistic treatment of TP-AGB stars in these models. The BaSTI isochrones also produce redder colors at young ages compared to the Padova isochrones, which is probably due a lack of convective core overshooting in the BaSTI isochrones adopted herein (see Figure 1). The data do not definitively favor one model over another at $\log(t/\text{yrs}) \lesssim 8.0$.

The disagreement in $V-I$ between the models and data at intermediate ages is also noteworthy. The models perform better at old ages, although it is unclear if this is because of the old ages or the lower metallicities of the old star clusters. We will return to issues with $V-I$ colors in later sections.

FSPS model predictions using the Padova isochrones are explored further in Figure 3. In this figure we compare the unmodified Padova isochrones to the modified model, and we also show the effect of a variation in metallicity of ± 0.2 dex about the modified model. For ages and colors this variation

with metallicity does not bracket the modified model because some metallicity-color relations in the models are not monotonic and in fact some colors are reddest at approximately the average metallicity of the LMC ($\log(Z/Z_{\odot}) \approx -0.3$). It is clear that use of the unmodified Padova models results in substantial disagreement with observed star clusters. This disagreement is driven to a significant extent by the large population of luminous carbon stars predicted in the Padova calculations. In our modifications to the Padova models we have substantially lowered the bolometric luminosity along the TP-AGB phase, which has the effect of down-weighting the importance of all TP-AGB stars, including carbon stars.

It is worth discussing in more detail the substantial disagreement between the unmodified Padova calculations and the star cluster data. The Padova group provided comparisons between their model and observations in Marigo et al. (2008) for $V-K$ and $J-K$ colors, finding acceptable agreement. The explanation for this difference is twofold.

First, the data used in their comparison is the old Persson data, which suffers from the issues discussed above. Second, and perhaps as important, the conversion from L_{bol} and T_{eff} to SEDs was achieved with the theoretical atmosphere models of Loidl et al. (2001) coupled to dust radiative transfer models from Groenewegen (2006). Aside from the fact that the dust models were never demonstrated to fit the $V-K$ colors of AGB stars, the Loidl et al. (2001) carbon star models are substantially bluer (by > 1 mag in $V-K$) than observed car-

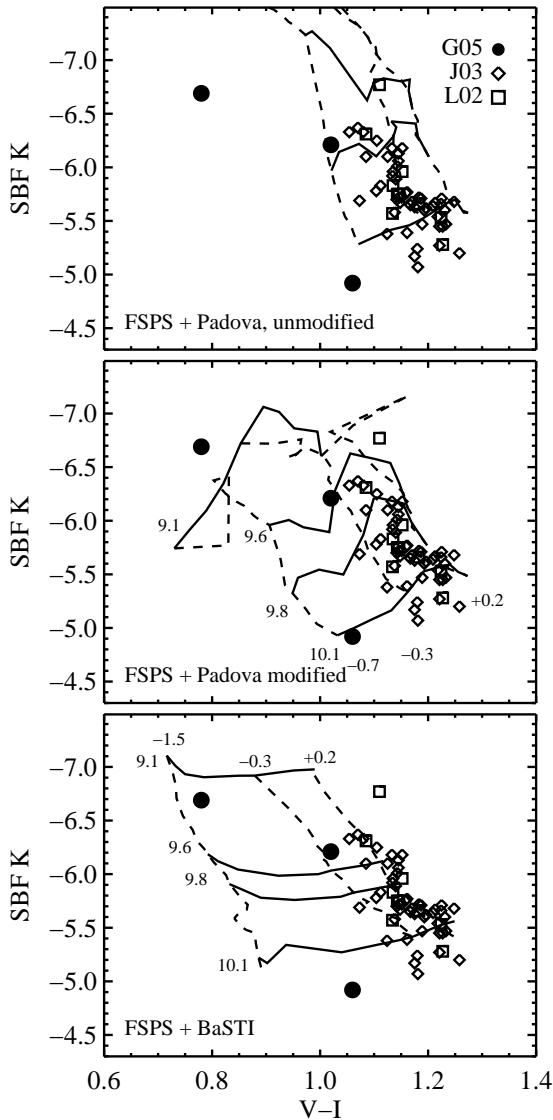


FIG. 5.— K -band SBFs as a function of integrated $V-I$ color. Model predictions (*lines*) are compared to observations of star clusters in the MCs (González-Lópezlira et al. 2005, G05), Elliptical galaxies in the Fornax cluster (Liu et al. 2002, L02), and Ellipticals in a variety of environments (Jensen et al. 2003, J03). Model predictions are displayed as lines of constant age (*solid lines*; labeled in units of $\log(t/\text{yrs})$ in the figure) and lines of constant metallicity (*dashed lines*); labeled in units of $\log(Z/Z_{\odot})$ in the figure). The age-metallicity grids in the top two panels are the same. SSP models are constructed with the unmodified Padova isochrones (*top panel*), modified Padova isochrones (*middle panel*), and the BaSTI isochrones (*bottom panel*).

bon stars (R. Gautschy, private communication). We believe that our transformation to SEDs is more robust since we use observed TP-AGB spectra. Our qualitative conclusions are echoed by Gullieuszik et al. (2008) who compared the population of O-rich and carbon stars in the Leo II dwarf galaxy to the Padova models and found that the models predict substantially more, and substantially more luminous O-rich stars than are seen in that galaxy. Finally, the Padova group uses the carbon star luminosity function in the MCs as a constraint on their TP-AGB model, but this observable can only provide valuable insight if the star formation histories (SFHs) of the

MCs are known to high precision in the age range relevant for carbon star production ($\approx 10^{8.5} - 10^{9.15}$ yrs).

4.2.2. Surface brightness fluctuations

Figures 4 and 5 compare near-IR SBFs between several FSPS-based models and MC data. In Figure 4 the evolution of SBF magnitudes and SBF colors are compared to our FSPS model with both the BaSTI and Padova isochrones. We show results both for the unmodified and modified Padova isochrones. The BaSTI isochrones provide an acceptable fit to the K -band SBFs, but produce SBF colors that are somewhat too blue compared to the data. This implies that the AGB and TP-AGB temperatures are too hot in the BaSTI calculations.

The unmodified Padova results show similar discrepancies as seen in Figure 3. SBF magnitudes and colors are too bright and too red, which can be traced back to the over-abundance of carbon stars and the over-luminous TP-AGB evolutionary phase. As discussed earlier in §4.2.1, these problems are rectified by altering the overall luminosity and temperature of stars in the TP-AGB phase. These modifications result in SBF magnitudes and colors that are in better accord with the data, although K -band SBFs tend to be somewhat lower than the observations at intermediate ages.

In Figure 5 we compare models and data in K -band SBFs versus integrated $V-I$ colors. In addition to MC star cluster data we include data from Elliptical galaxies (Liu et al. 2002; Jensen et al. 2003). It is clear that the modified Padova isochrones span the range of data much better than the unmodified isochrones. In addition, notice that there is a subsample of Ellipticals that have SBFs fainter than predicted by the models. This has a direct and potentially important impact on the inferred mass-to-light ratios of these systems and consequently on their inferred stellar masses. SBFs in the red/near-IR will correlate inversely with derived stellar masses, and therefore if SBFs are overestimated in the models (as is the case here), then derived stellar masses will be underestimated.

The models shown in Figure 5 assume solar-scaled chemical compositions, while many Elliptical galaxies are α -enhanced (e.g., Worthey et al. 1992; Thomas et al. 2005). However, Lee et al. (2009a) have shown that the level of α -enhancement has almost no effect on the model predictions in the $V-I$ vs. $F160W$ SBF plane ($F160W$ is similar to the H -band), and therefore our conclusions should not be effected by these details.

4.3. Constraints from the MW & M31

4.3.1. Optical and near-IR colors

SPS model predictions for the metallicity-dependent optical and near-IR colors of old populations are compared to observed star clusters in Figure 6. Model predictions are restricted to ages of 12.5 Gyr, although results are not sensitive to this particular age. FSPS models with both the BaSTI and modified Padova isochrones are included, as are the predictions from M05 and BC03. Comparisons to star clusters in both the MW and M31 are included. For all colors except for $J-K$ the MW and M31 data agree (see below), although the scatter in M31 cluster colors is larger. This is probably due to the effects of internal reddening in M31 that has not been accounted for.

The models reproduce the trends in the observed colors fairly well, although there are areas of noteworthy disagreement. The $U-V$ and $B-V$ colors are somewhat too blue

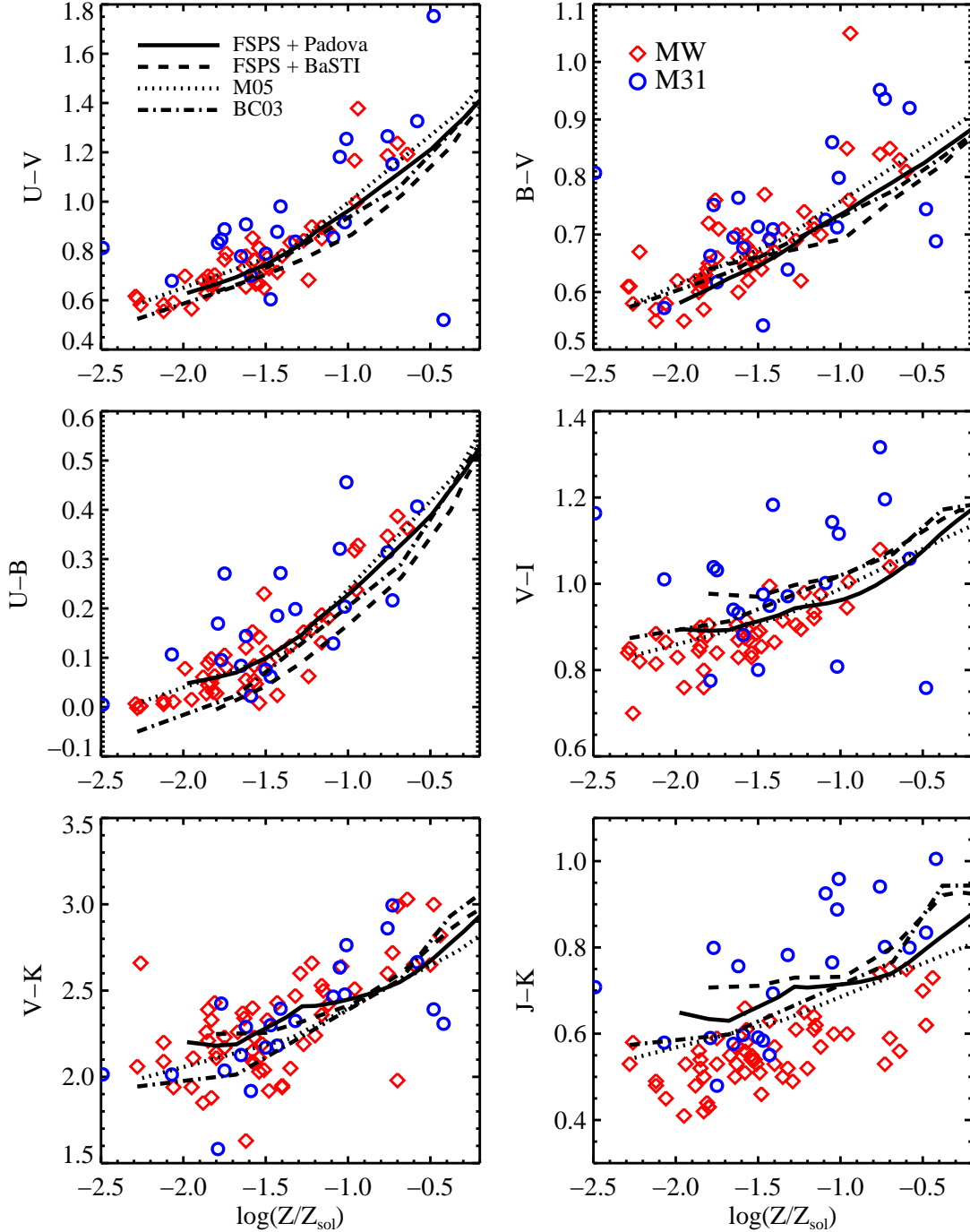


FIG. 6.— SSP colors as a function of metallicity, for old ages ($t \approx 13$ Gyr). Model predictions are compared to observations of globular clusters in the MW and M31. The model SSPs include the predictions from M05 (dotted lines), BC03 (dot-dashed lines), and predictions from the present work where either the Padova or BaSTI stellar evolution calculations have been assumed. In general the agreement between models and data is acceptable, though the data tend to be redder than the models as the metallicity increases. The difference in $J-K$ color between MW and M31 star clusters is striking.

in the models at $\log(Z/Z_{\odot}) > -1.0$. The FSPS model with the BaSTI isochrones perform worst of the models considered. We can check whether or not this general disagreement between models and data in UBV filters is due to the adopted spectral library by considering the empirical Miles stellar spectral library. Due to the limited wavelength range of this library, we can only construct the $B-V$ color. The

$B-V$ colors from the Miles empirical library are almost indistinguishable from the colors using the BaSeL library, implying that the stellar atmospheres are not the source of the discrepancy. A similar test was performed in BC03, where they compare the BaSeL, STELIB, and Pickles (1998) libraries and find negligible differences in $B-V$ at $Z = Z_{\odot}$.

A second possible explanation for the differences between

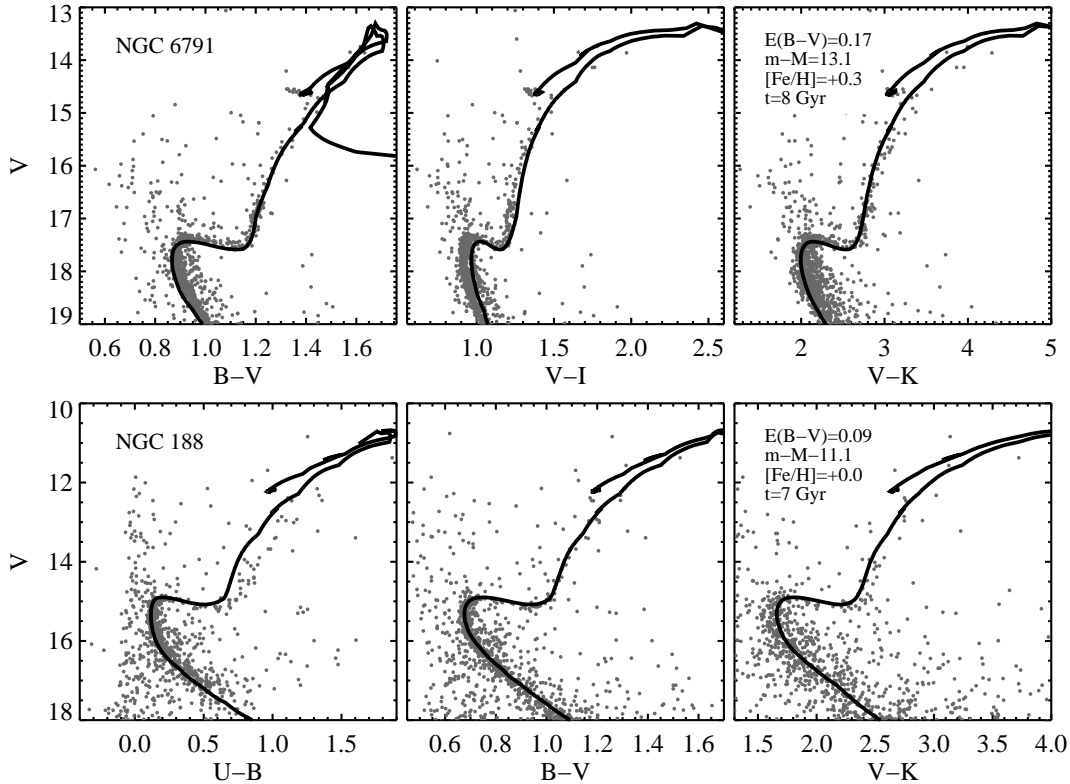


FIG. 7.— CMDs for two metal-rich MW star clusters, NGC 6791 (*top rows*) and NGC 188 (*bottom rows*), compared to FSPS model predictions using the BaSTI isochrones. Notice the strong BS population above the main sequence turn-off for both NGC 6791 and NGC 188. The adopted cluster parameters are shown in the legends.

models and observations in the $U-V$ and $B-V$ colors is the UBV filter transmission curves. The B filter used for these data actually consist of two slightly different filters (see the discussion in Maraston 2005). It is difficult to determine which filter was used in each observation. The difference between these two filters varies from 0.02 to 0.04 mags. The $U-V$ color is constructed by adding the $U-B$ and $B-V$ colors, so this color will also be subject to this source of uncertainty. The offsets between models and data is of order 0.05 mags — the same order as the differences induced by the two B filters — and so we cannot make stronger comparisons between models and data until more reliable optical photometry is available for MW and M31 star clusters.

The morphology of the HB cannot explain the observed discrepancy because in all SPS models shown in Figure 6 adopt a red HB at $\log(Z/Z_{\odot}) > -1.0$. The HB therefore cannot be modified to produce even redder model colors.

The model $V-I$ colors compare favorably with the data at $\log(Z/Z_{\odot}) > -1.0$. At lower metallicities the models diverge from the data, with the FSPS model using BaSTI isochrones performing worst.

All models fail at predicting the observed $V-K$ and $J-K$ colors, both at low and high metallicities for the latter and at higher metallicities for the former. Recall that the near-IR data comes from a recent analysis of 2MASS data by Cohen et al. (2007). Our results echo those of Cohen et al. (2007) who compared MW star cluster $J-K$ colors against several SPS models. In addition to the M05 model, they also compare to the models of Worthey (1994) and Buzzoni (1989)

and find similar levels of disagreement with these other models.

Cohen et al. (2007) speculate that the cause of the discrepancy could be either 1) inadequate calibration of the stellar libraries or 2) issues with the near-IR filter transmission curves (Cohen et al. used published predictions for Johnson JHK photometry from these models). Since we compute 2MASS magnitudes self-consistently from the model spectra, the second explanation cannot be the source of the discrepancy. The problem is not likely to be due to inadequacies in the theoretical stellar spectral libraries, since the colors of giants compare well with observed stars in the near-IR (Westera et al. 2002). The temperature of the RGB need only be lowered by 200K in order to achieve better agreement in $V-K$ (although a lower RGB temperature would only exacerbate the disagreement in $J-K$). As explored in §4.3.2, one need only change the RGB at the brightest ~ 1 mag to in order to produce substantial changes in $V-K$ colors. Without definitively identifying the source of this problem, we are forced to simply reiterate the conclusions of Cohen et al. that near-IR colors of old populations cannot be used to constrain the metallicities or ages of either GCs or distant galaxies.

It should also be noted that the near-IR photometry presented in Cohen et al., which is based on data from the 2MASS survey, differs substantially from previous near-IR photometry of MW clusters provided by M. Aaronson et al. (1977; unpublished). The differences in $J-K$ are 0.1–0.2 mags in the sense that the latest results are bluer than the older data. Since previous models were calibrated against the older

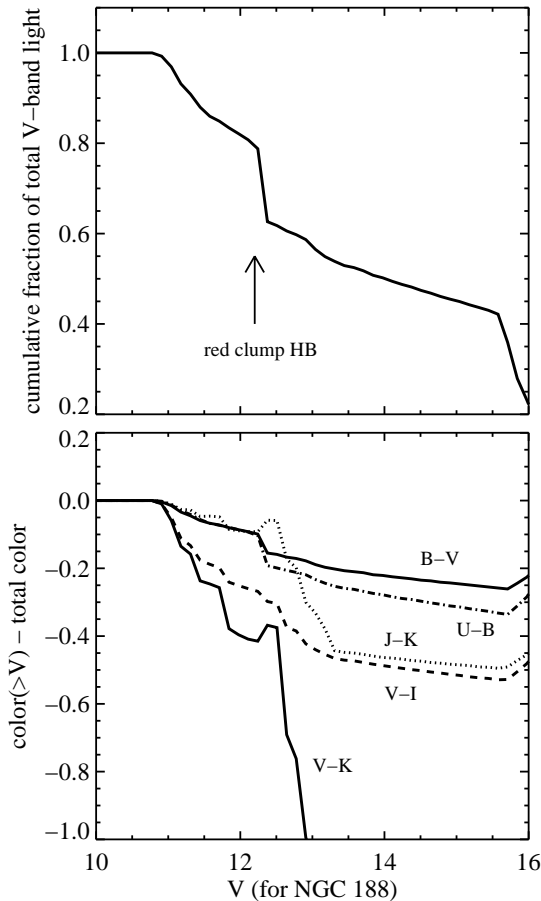


FIG. 8.— *Top panel*: Cumulative fraction of V -band light as a function of apparent V -band magnitude for a 7 Gyr SSP with $[\text{Fe}/\text{H}] = +0.0$. The apparent V -band magnitude along the x -axis is scaled by the distance modulus and reddening value appropriate for the star cluster NGC 188 shown in Figure 7. Red clump HB stars appear at $V \sim 12$. *Bottom panel*: Integrated color for all stars fainter than V , normalized to the integrated color for all stars. The model SSP is the same as in the top panel. Integrated colors in the red and near-IR can only be constrained from CMDs if the very brightest and rarest stars in the cluster are identified.

data (e.g., Maraston 2005), it is not surprising that the models are all redder than the Cohen et al. data.

The most dramatic discrepancy in Figure 6 is between the $J-K$ colors in MW and M31 star clusters. The M31 clusters are approximately 0.2 mags redder in $J-K$ than the MW clusters. Internal reddening in M31 cannot be the source of this discrepancy because reddening effects are quite small in $J-K$, especially in comparison to the colors considered in Figure 6, which do not show such an offset. Barmby et al. (2000) have also presented JHK photometry of old M31 star clusters. Their results are consistent with the M31 results from the RBC catalog shown in Figure 6, suggesting that the discrepancy in $J-K$ is not due to data reduction issues. We cannot provide a compelling explanation for this discrepancy, but note that without an explanation it is impossible to calibrate the old metal-poor models to better than ~ 0.2 mags in the near-IR.

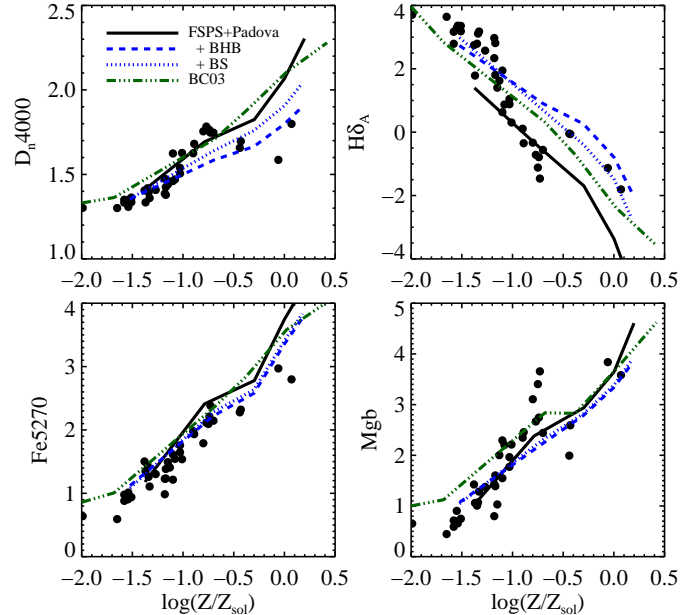


FIG. 9.— Spectral indices versus metallicity for old populations. Indices are derived from the integrated spectra of MW star clusters presented in Schiavon et al. (2005, *symbols*), and are compared to indices of SSPs at $t = 10$ Gyr for several SPS models. Here, our FSPS model uses Padova isochrones and the empirical Miles stellar library. Additional FSPS predictions that include a fraction of blue HB stars ($f_{\text{BHB}} = 0.5$) and BS stars ($S_{\text{BS}} = 2$) are shown. The BaSTI isochrones (not shown), are similar in most respects to the Padova isochrones, except for the metal-poor $H\delta_A$ strengths, which are larger in the BaSTI models because of a bluer HB. The model predictions of BC03 are also included in the figure.

4.3.2. Metal-rich CMDs

Calibrating data at higher metallicities than shown in Figure 6 is far more desirable from the standpoint of using SPS to model galaxies since galaxies are generally of higher metallicity. Unfortunately, old metal-rich star clusters are rare. Classic metal-rich clusters include NGC 6791, NGC 188, NGC 6553, and NGC 6528; the latter two belong to the bulge and thus are along sightlines of high extinction.

In Figure 7 we compare multi-color CMDs of NGC 6791 and NGC 188 to our SPS predictions. The consideration of multi-color CMDs provides a powerful constraint on SPS models in part because the reddening value cannot be arbitrarily varied to fit a color without potentially worsening the fit at another color. NGC 188 and 6791 are open clusters in crowded fields and therefore CMD construction is challenging without radial velocities and/or proper motions to isolate true members. This complication should be kept in mind when considering model comparisons below.

NGC 6791 is assumed to have an age of 8.5 Gyr, $E(B-V) = 0.17$, $[\text{Fe}/\text{H}] = +0.4$, $[\alpha/\text{Fe}] = 0.0$, and $m-M = 13.0$ (Carney et al. 2005; Origlia et al. 2006; Kalirai et al. 2007). JK and BVI photometry are provided by Carney et al. (2005) and Stetson et al. (2003), respectively. The cluster parameters for NGC 188 are taken to be $E(B-V) = 0.09$, $[\text{Fe}/\text{H}] = -0.06$, $[\alpha/\text{Fe}] = 0.0$, $m-M = 11.1$, and an age of 7 Gyr (Sarajedini et al. 1999; Carretta et al. 2009). $UBVRI$ photometry of this cluster is provided by Sarajedini et al. (1999); near-IR photometry is extracted directly from the 2MASS

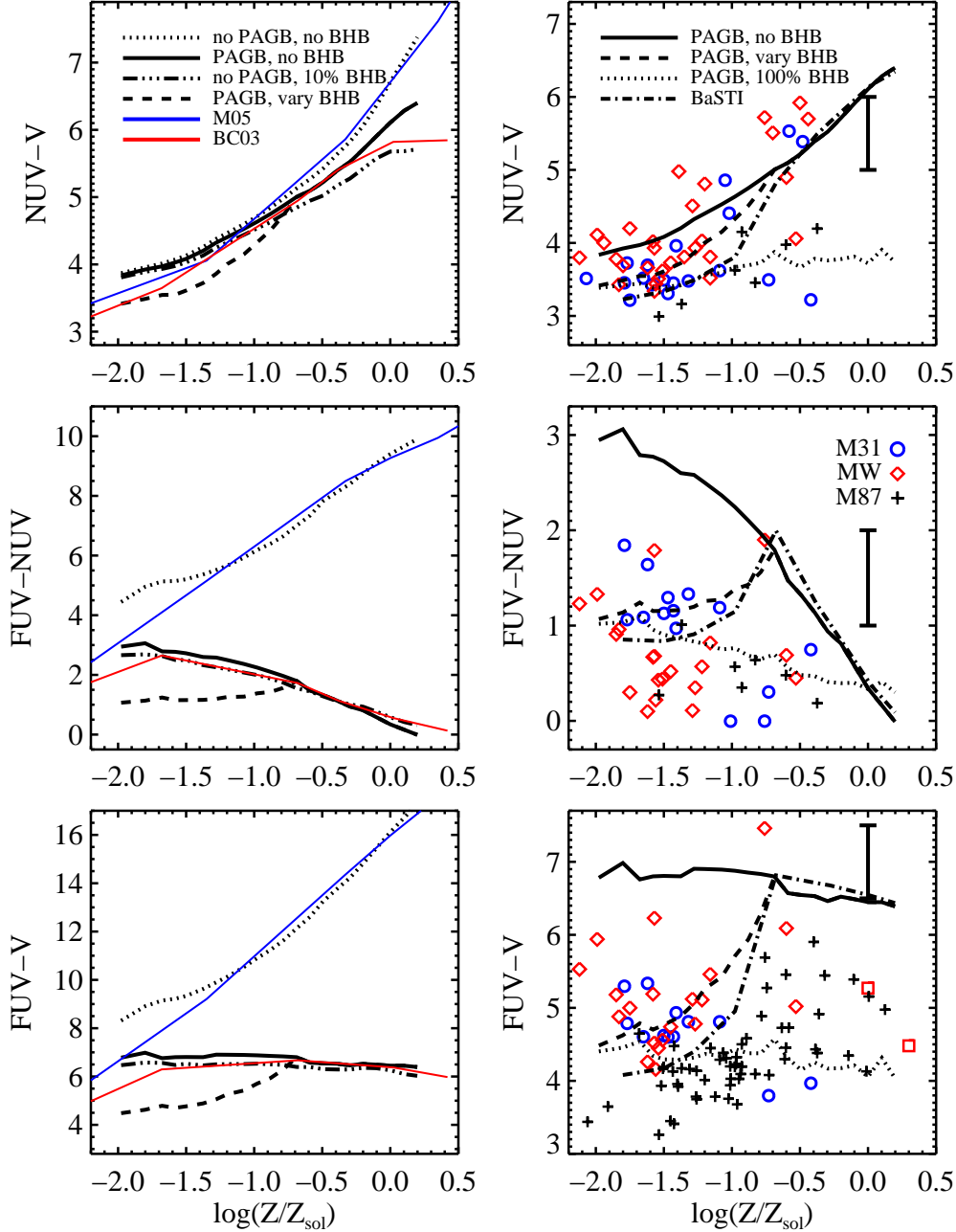


FIG. 10.— SSP UV colors as a function of metallicity, for old populations ($t \approx 13$ Gyr). Model predictions are compared to observations of star clusters in M31 (Rey et al. 2007), the MW (Dorman et al. 1995), and M87 (Sohn et al. 2006). A variety of models are considered to explore the effects of post-AGB (PAGB) stars and blue HB (BHB) stars. These models, which are described in detail in the text, are constructed with the Padova isochrones. Model predictions from M05, BC03 are also included, as is a model with the BaSTI isochrones. In addition, the approximate location of Elliptical galaxies from the SAURON survey (Jeong et al. 2009) are included in the right set of panels as error bars at $\log(Z/Z_{\odot}) = 0.0$. Approximate locations of two metal-rich MW star clusters NGC 188 and NGC 6791 are shown as open squares (see Sohn et al. 2006). Notice the different y-axes in the left and right panels.

point source catalog¹⁰.

We use the BaSTI isochrones for the following comparisons because those isochrones have been computed for $\log(Z/Z_{\odot}) = +0.3$, which is comparable to the metallicity of NGC 6791 and is higher than the highest metallicities avail-

¹⁰ The 2MASS point source catalog was queried using the NASA/IPAC Infrared Science Archive, available at <http://irsa.ipac.caltech.edu/applications/Gator/>.

able from the Padova isochrones. Our model CMDs are compared to NGC 6791 and NGC 188 in Figure 7 for the same reddening values, ages, and distance moduli as quoted above, but for slightly different metallicities. Metallicities of $\log(Z/Z_{\odot}) = +0.3$ for NGC 6791 and $\log(Z/Z_{\odot}) = +0.0$ for NGC 188 are adopted based on the available isochrones.

The agreement between data and models is generally good, including the location of the main sequence turn-off, the sub-giant branch and RGB, and the position of the red HB.

The model fails to reproduce the low mass end of the main sequence in NGC 6791 in the sense that the model isochrone is on the blue side of the data in $B-V$ and $V-K$ and on the red side in $V-I$. Of course, this disagreement is of little consequence for integrated properties since low mass stars are faint. The disagreement at low masses is probably due to uncertainties associated with color- T_{eff} relations for low-mass stars at high metallicity (Cassisi et al. 2000; Cassisi 2007). It appears that the model RGB $V-K$ color becomes progressively bluer than the RGB of NGC 6791 at higher luminosities, although it is difficult to make firm statements owing to the paucity of data at the bright end. Notice that this discrepancy is in the same sense as was seen for integrated $V-K$ colors of metal-poor MW and M31 clusters (see §4.3.1).

The model CMDs perform well when compared to NGC 188. The only obvious discrepancy is in the $U-B$ color of the RGB. Thankfully, this is of little consequence for integrated colors because the integrated $U-B$ color is determined primarily by the main sequence turn-off point and sub-giant branch, not the RGB (see below).

For the purpose of modeling entire galaxies, we are interested in the ability of SPS models to accurately predict the *integrated* colors of star clusters. It is therefore worth considering the extent to which constraints from resolved CMDs can constrain integrated colors of clusters.

In Figure 8 the integrated colors corresponding to the CMD of NGC 188 are explored. Integrated colors are computed by including all stars fainter than a given apparent V -band magnitude. It is clear from this figure that integrated blue colors such as $U-B$ and $B-V$ are well constrained even at relatively faint magnitudes in V . This occurs because integrated blue colors are determined primarily by the main sequence turn-off point and sub-giant branch. In contrast, redder and near-IR colors are highly sensitive to the brightest one magnitude ($11 < V < 12$) for the simple reason that the RGB and AGB dominate the near-IR light. The brightest one magnitude in V contributes $\approx 20-40\%$ of the integrated V -band light (depending on whether or not one includes the red clump HB), and the $V-I$ and $V-K$ colors redden dramatically in this brightest magnitude. Thus, unless the brightest, and rarest stars in clusters can be reliably identified and used for model calibration, model constraints in CMD-space will not guarantee accurate model integrated colors.

4.3.3. Spectral indices

We now turn to an analysis of the spectral indices of old populations over a range of metallicities. Observed indices are measured from the catalog of optical spectra for 40 MW star clusters from Schiavon et al. (2005). The indices are measured in the exact same way for both the observed spectra and the models, ensuring reliable comparison. The FSPS model spectra are at slightly higher resolution than the MW cluster spectra, so the model spectra have been broadened to match the resolution of the data. The spectral resolution of the BC03 model is comparable to the observed spectra, and so the BC03 model spectra were not broadened.

Figure 9 presents the spectral indices D_n4000 , $H\delta_A$, Fe5270, and Mgb as a function of metallicity for the Schiavon et al. sample and the FSPS and BC03 SPS models. The FSPS predictions utilize the Miles empirical stellar library, while BC03 adopt the STELIB empirical library. For these ages the Padova predictions are very similar to the BaSTI isochrones except for $H\delta_A$ at low metallicity because the BaSTI isochrones have a hotter HB. This figure also demon-

strates the importance of BS stars and an extended/blue HB by including models with $S_{\text{BS}} = 2$ and $f_{\text{BHB}} = 0.5$ (see §3.1).

There are several important conclusions to draw from this figure. First, the models are able to reproduce the observed metallicity dependence of the Mgb and Fe5270 indices over the full observed range. At low metallicities this success is driven largely by the fact that the bulk of the metal-poor stars in the empirical stellar library contains α -enhanced stars (Milone et al. 2009). While the isochrones used in FSPS are solar-scaled¹¹, recent work has shown that for old populations the effects of α -enhancement are strong on the stellar libraries and weak on the isochrones (Schiavon 2007; Lee et al. 2009c,b).

The default SPS models (i.e., without BS or blue HB stars) predict D_n4000 in excess of observed values at solar metallicity, and the same models predict $H\delta_A$ strengths too weak compared to the observations at both very low and solar metallicity. The disagreement at matching $H\delta_A$ at very low metallicity is a consequence of the well-known fact that most low metallicity clusters have a blue HB. Indeed, the models do a better job of matching the observed $H\delta_A$ strengths at low metallicity for $f_{\text{BHB}} > 0.5$.

The failure of the models for both D_n4000 and $H\delta_A$ at solar metallicity is more striking, and has potentially significant consequences for understanding the spectra of metal-rich galaxies. The two solar metallicity clusters are NGC 6553 and NGC 6528; both are in the bulge. The CMD of NGC 6553 shows an abundance of BS stars (Zoccali et al. 2001), and so the addition of such stars to the models in Figure 9 is justified. Indeed, adding BS stars results in much better agreement in $H\delta_A$ and moderately better agreement for D_n4000 . The addition of blue HB stars also alleviates much of the discrepancy between models and data. Lee et al. (2009b) compare their model to the same dataset and find that for solar-scaled models the $H\delta_A$ strengths are too weak compared to the observed $Z \approx Z_{\odot}$ clusters, echoing our results regarding our default SPS model.

Main sequence turn-off stars are the dominant stellar phase controlling the strength of D_n4000 . The effective temperature of turn-off stars would have to be increased by $\sim 1000\text{K}$ in order to alleviate the discrepancy at solar metallicity. Such an increase would yield a CMD in gross conflict with observations. Modifications to the standard stellar phases thus cannot reconcile the data and model D_n4000 strengths. Either BS, blue HB stars or both are therefore the most likely candidates for explaining the discrepancy.

4.3.4. Ultraviolet colors

In the absence of evolved or young stars, the ultraviolet is sensitive to the temperature of main sequence turn-off stars. Since the temperature of turn-off stars depends on metallicity at fixed age, ultraviolet colors such as $NUV-V$ and $FUV-V$ will, in the absence of evolved or young stars, redden substantially with increasing metallicity.

In reality, the interpretation of ultraviolet colors of old populations is complicated by the existence of hot, evolved stars, including post-AGB, extended/blue HB, and BS stars (e.g., Burstein et al. 1988; Greggio & Renzini 1990; Dorman et al. 1995; O’Connell 1999; Brown et al. 2000; Han et al. 2007). It is beyond the scope of this paper to consider in detail the constraints on the relative importance of these various popu-

¹¹ Although recall that the BaSTI database does provide α -enhanced stellar evolution models.

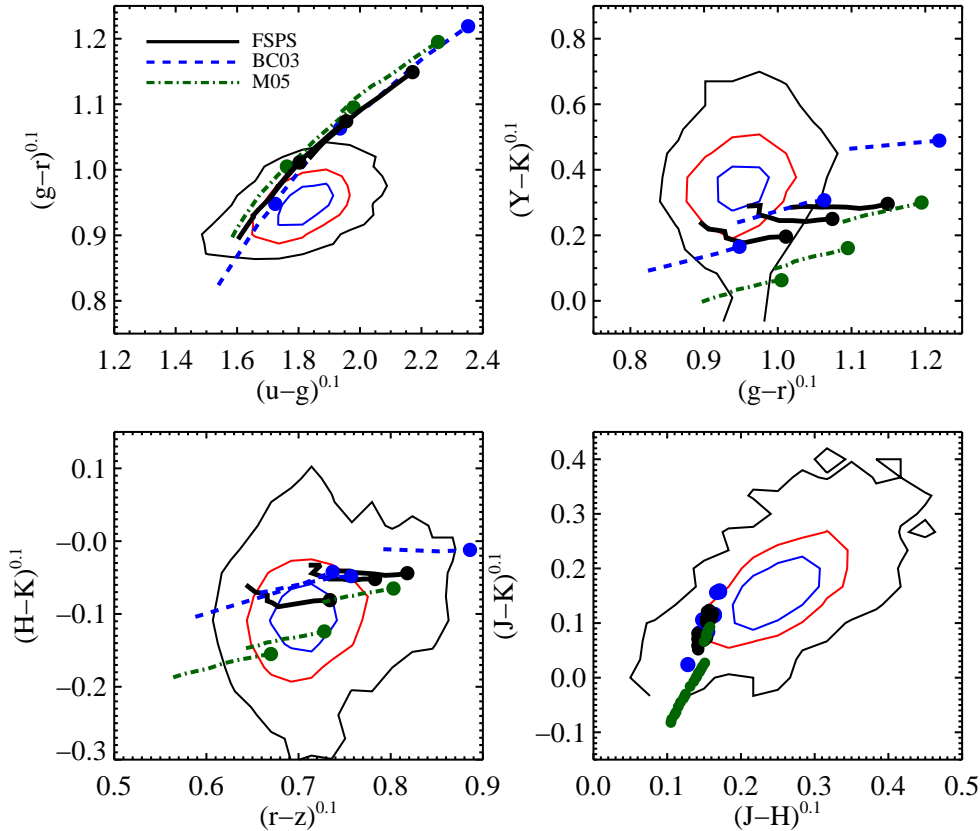


FIG. 11.— Color-color diagrams comparing observed luminous red sequence galaxies to both our FSPS model with the modified Padova isochrones, and the models of BC03 and M05. The contours enclose 40%, 68%, and 95% of the observed galaxies. For each model, the colors of dust-free SSPs are plotted for ages $5 < t < 13$ Gyr for three metallicities: $\log(Z/Z_{\odot}) \approx -0.2, 0.0, 0.2$ (corresponding to three lines for each model). Symbols mark the location of $t = 13$ Gyr for each metallicity. In the lower right panel, all model predictions are shown as symbols for clarity.

lations afforded by ultraviolet colors. Instead, our goal will be to demonstrate that plausible variations in the relative weights assigned to post-AGB and blue HB stars can explain the ultraviolet properties of observed star clusters.

Ultraviolet colors of star clusters in M31 (Rey et al. 2007), the MW (as compiled by Dorman et al. 1995), and M87 (Sohn et al. 2006) are compared to SPS models in Figure 10. The approximate location of Elliptical galaxies from the SAURON survey (Jeong et al. 2009) are also included in the figure. We include model predictions from our FSPS code for both the Padova and BaSTI isochrones, along with model predictions from BC03 and M05. Recall that M05 does not include post-AGB stars and so the FUV photometry, which is sensitive to such hot stars, cannot be reliably compared to the data. M05 does include blue HB stars for metal-poor models. BC03 includes post-AGB stars but does not include blue HB stars at any metallicity.

For the FSPS predictions with the Padova isochrones, we include several model variations. In particular, we consider models 1) without post-AGB and without blue HB stars; 2) with post-AGB but without blue HB stars; 3) without post-AGB stars and with a blue HB fraction of 10%; 4) with post-AGB stars and a blue HB fraction of 100%; 5) with post-AGB stars and a blue HB fraction that varies with metallicity as $f_{\text{BHB}} = -0.75 \log(Z/Z_{\odot}) - 0.5$ for $\log(Z/Z_{\odot}) < -0.7$ and zero otherwise.

Before considering the insights gained from model comparisons, it is worth drawing attention to the considerable vari-

ation in observed ultraviolet colors of star clusters at fixed metallicity. $NUV - V$ colors vary by ≈ 0.5 mags at fixed Z , while $FUV - V$ varies by > 1 mag. This phenomenon is known as the ‘second-parameter’ effect, and has been known for decades (see the review in Catelan 2009). Parameters that might be responsible for the additional variation at fixed Z include age, helium content, mass-loss, stellar rotation, and magnetic fields. The particular solution is not as important as the observed variation. It is difficult to imagine constraining an SPS model in the UV given these variations, and it will therefore continue to be very challenging to extract useful information from the UV flux of quiescent galaxies.

The locus of ultraviolet colors of Elliptical galaxies do not correspond to star clusters of any metallicity in either M31, the MW, or M87. The $NUV - V$ colors correspond to metal-rich clusters, while the $FUV - NUV$ colors are similar to metal-poor clusters, and the $FUV - V$ colors of the Elliptical sample are significantly redder than any star cluster. This conflict may be due in part to the fact that galaxies are not mono-metallic. The ultraviolet is quite sensitive to metallicity, and so accurate modeling of the metallicity distribution function is essential for these objects. These and related issues regarding stellar population modeling of Ellipticals will be discussed in §4.4–4.5.

It should also be noted that the star clusters in M87 are significantly bluer in ultraviolet colors at fixed metallicity compared to clusters from the MW and M31. The source of this difference is not known, although differences in cluster age

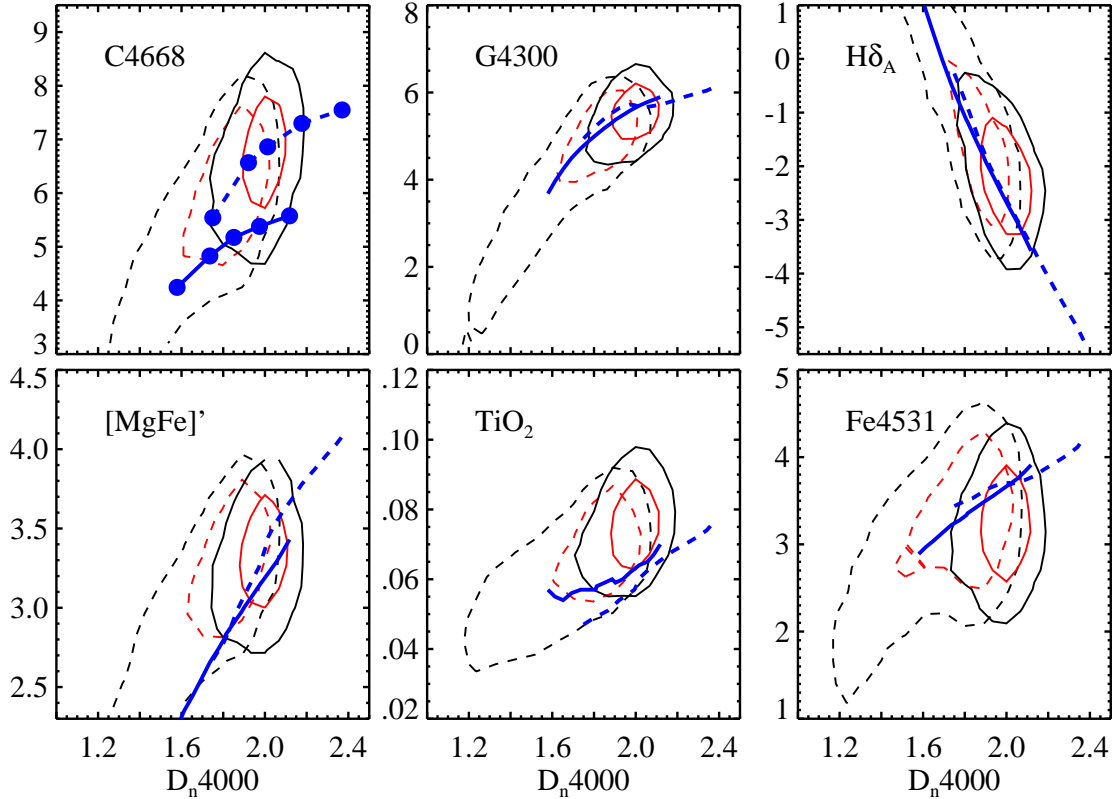


FIG. 12.— Comparison of spectral indices for a sample of SDSS galaxies (68% and 95% contours) to our FSPS model predictions (lines). Here, our FSPS model uses the empirical Miles stellar library and the Padova isochrones. SDSS galaxies are divided by $\sigma > 200 \text{ km s}^{-1}$ (solid contours) and $100 < \sigma < 200 \text{ km s}^{-1}$ (dashed contours). Model predictions are displayed for dust-free SSPs with metallicities of Z_{\odot} (solid lines) and $1.5Z_{\odot}$ (dashed lines) for $2 < t < 13 \text{ Gyr}$. Model spectra are Doppler broadened to $\sigma = 200 \text{ km s}^{-1}$. In the upper left panel, symbols denote ages of 2.2, 3.5, 5.6, 8.9, 14.1 Gyr, in order of increasing D_n4000 .

or helium abundance are possible explanations (Sohn et al. 2006; Kaviraj et al. 2007). Nevertheless, it is clear that even if models can be constructed that match the MW cluster data, such models may not be applicable to other systems.

Several conclusions can be drawn from the comparisons between models and data. First, a 10% blue HB fraction at all metallicities produces ultraviolet colors that are comparable to post-AGB stars, demonstrating the degeneracy between these two evolutionary phases when considering UV colors. The BaSTI isochrones and the Padova isochrones with variable blue HB fraction are both able to fit a majority of the metallicity-dependent ultraviolet data. At metallicities $\log(Z/Z_{\odot}) > -0.7$ these models fail to reproduce the observed FUV fluxes, whereas models with 100% blue HB fractions can reproduce this data.

When modeling the ultraviolet flux of galaxies, a flexible treatment of hot evolved stars is clearly warranted given our inadequate theoretical understanding of the observed ultraviolet colors of clusters, and given the considerable scatter in observed ultraviolet data at fixed metallicity.

4.4. Constraints from quiescent galaxies

We now consider constraints on SPS models provided by massive red sequence, (i.e., quiescent), galaxies. Such galaxies are thought to be composed primarily of old ($t > 10 \text{ Gyr}$), metal-rich stars.

4.4.1. Colors

Figure 11 compares galaxies to models in color-color space. We include the FSPS model predictions with the modified Padova isochrones in addition to the BC03 and M05 models.

All models predict similar ugr colors. One clearly sees the almost perfect degeneracy between age and metallicity in this color-color space. It is also clear that all models predict ugr colors that are substantially redder than the data, assuming that such galaxies are composed of old, metal-rich stars (e.g., Worthey et al. 1992; Trager et al. 2000; Thomas et al. 2005; Graves & Schiavon 2008). The discrepancy between observed and predicted $g-r$ colors is $\gtrsim 0.1 \text{ mags}$. Potential remedies to this discrepancy are explored in §4.5.

The models perform reasonably well in the near-IR, although there is a notable disagreement in the $J-H$ color for all models. In the $r-z$ vs. $H-K$ plane the FSPS and M05 models perform well, while BC03 fits the data only for solar or sub-solar metallicities. The BC03 and M05 models predict strong variations in $Y-K$ with metallicity, in contrast to FSPS. Given the narrow distribution of observed $Y-K$ colors, the BC03 models would predict nearly all red sequence galaxies to be solar metallicity, while M05 would predict that all were super-solar. In contrast, FSPS allows for a range of metallicities from sub- to super-solar, in better agreement with detailed analysis of the spectra of red sequence galaxies (e.g., Thomas et al. 2005).

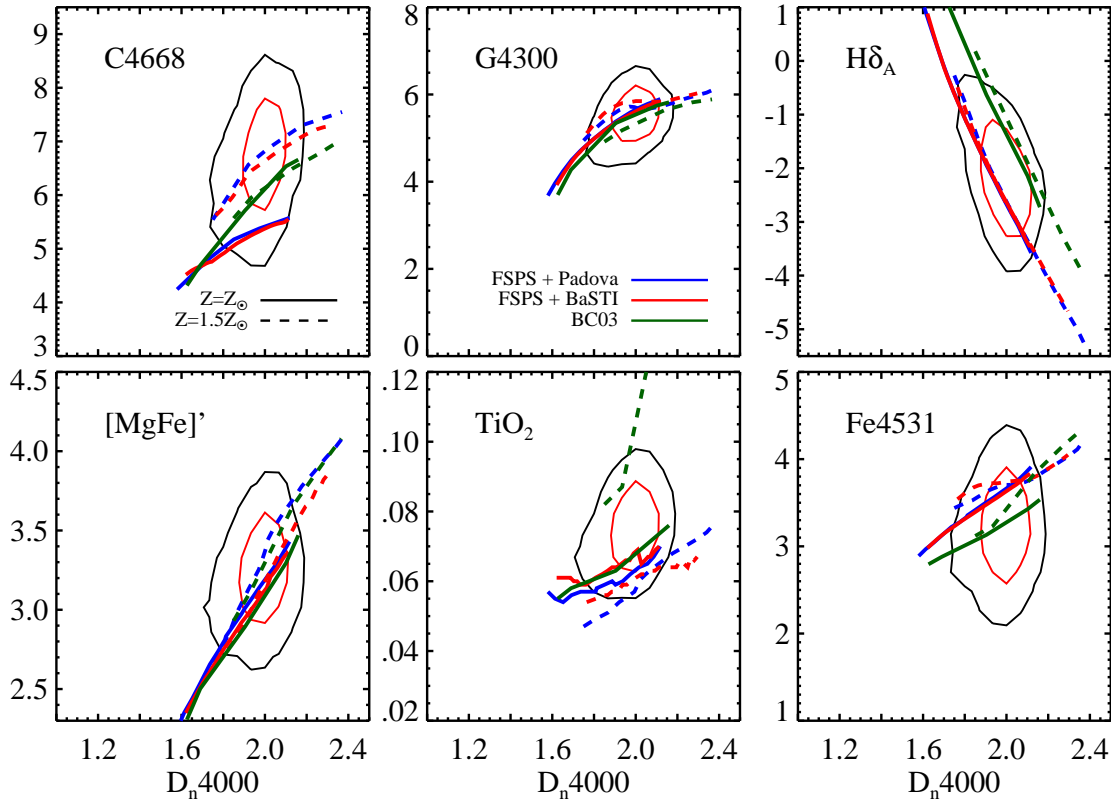


FIG. 13.— Spectral indices for a sample of SDSS galaxies with $\sigma > 200 \text{ km s}^{-1}$ (contours), compared to several models for dust-free SSPs. FSPS model predictions are shown for both the Padova and BaSTI isochrones where in each case the empirical Miles stellar library is used in the model construction. Predictions from the BC03 model are also included. Models are shown for metallicities of Z_{\odot} (solid lines) and $1.5Z_{\odot}$ (dashed lines) and for ages in the range $2 < t < 13$ Gyr. Model spectra are Doppler broadened to $\sigma = 200 \text{ km s}^{-1}$.

Perhaps the most important conclusion to be reached from these color-color comparisons is that no model is able to reproduce the observed locus of red galaxies for all near-IR colors, and in addition no model can match the locus of galaxies in the $u-g$ vs. $g-r$ plane.

It should also be noted that within the context of one model, optical and near-IR color combinations, in particular $g-r$ vs. $Y-K$, are in principle capable of breaking the age-metallicity degeneracy. In practice it is not currently possible to use such colors to break this degeneracy for the twofold reason that the models cannot predict the observed locus of galaxies in that space and the models do not compare well with each other (see also Eminian et al. 2008; Carter et al. 2009).

The red and near-IR colors of these galaxies are determined primarily by the RGB. As noted in §4.3.2, resolved CMDs do not help constrain model predictions for integrated red and near-IR colors because these colors are determined by the brightest and rarest RGB stars. Homogeneous, integrated near-IR photometry for a sample of old metal-rich clusters would be invaluable for constraining models in this regime.

4.4.2. Spectral indices

Figure 12 compares spectral indices of SDSS galaxies to the FSPS model constructed with the Padova isochrones and the Miles empirical stellar library. The data are split according to their velocity dispersions. All models in this section are broadened to $\sigma = 200 \text{ km s}^{-1}$ in order to compare to the more

massive data bin. Model predictions are shown for dust-free SSPs at $Z = Z_{\odot}$ and $Z = 1.5Z_{\odot}$ for ages $2 < t < 13$ Gyr.

The index D_n4000 , which measures the strength of the CaII lines and the balmer decrement, is often taken to be sensitive primarily to age, and this is borne out in the figure. The majority of the other indices are sensitive to a combination of age and metallicity. The index C4668, which is a blend of many metallic lines including Fe, Ti, Cr, Mg, Ni, and C_2 (Worthey et al. 1994), is the most sensitive to metallicity of the indices shown, at fixed D_n4000 . The index $[MgFe]'$ was defined by Thomas et al. (2003) in order to be insensitive to α -enhancement. The G4300 index is sensitive to both CH and FeI (Worthey et al. 1994). $H\delta_A$ is often used to constrain the fraction of recent star formation because of its sensitivity to A stars (e.g., Kauffmann et al. 2003), and so the reliability of SPS models in the $H\delta_A - D_n4000$ plane is particularly important. For old populations, the interpretation of $H\delta_A$ is complicated by the presence of nearby absorption due to the CN molecule. This implies that the $H\delta_A$ index can be sensitive to non-solar abundance ratios, depending on the precise definition of the index (Prochaska et al. 2007). The trend is such that increasing α -enhancement will result in a weaker measured $H\delta_A$ index because the flux redward of the line will be depressed due to increased CN absorption.

Figure 13 compares several SPS models to the $\sigma > 200 \text{ km s}^{-1}$ SDSS sample. The BC03 model predictions are compared to the FSPS models using both the modified Padova

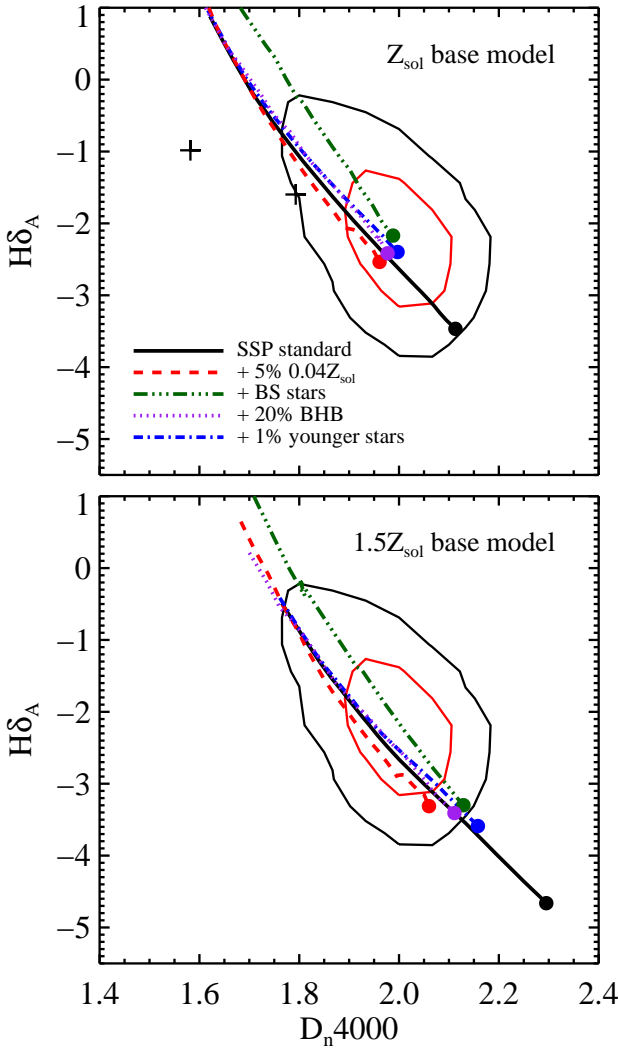


FIG. 14.— Comparison of the spectral indices D_n4000 and $H\delta_A$ between SDSS galaxies with $\sigma > 200 \text{ km s}^{-1}$ (contours) and various models constructed with FSPS adopting the Padova isochrones (as in previous figures). Model spectra are Doppler broadened to $\sigma = 200 \text{ km s}^{-1}$ and span the age range $2 < t < 13$ Gyr, with the oldest point marked by a solid symbol. Blue HB (BHB) stars, young stars (with an age of 1 Gyr), metal-poor stars, and BS stars (with $S_{BS} = 2$) are considered as additions on top of a base dust-free SSP of either solar or super-solar metallicity. The locations of two $\sim Z_\odot$ MW bulge star clusters are included (crosses) from the integrated spectra of Schiavon et al. (2005). The MW star cluster spectra were Doppler broadened to $\sigma = 200 \text{ km s}^{-1}$ for comparison to the galaxy data.

and BaSTI isochrones with the Miles empirical stellar library. The M05 model is not included because the spectral library in that model (The Kurucz library) is not of sufficient resolution to measure these indices.

The BaSTI and Padova isochrones have very similar main sequence turnoff points at old ages (see Figure 1). The primary difference between these isochrones is that the BaSTI RGB is approximately 100K hotter than the Padova RGB. Blueward of $\lambda = 5000 \text{ \AA}$ the main sequence and sub-giant branch dominate the flux, and so one would expect very little differences in spectral indices between these two isochrone sets in the blue, for a fixed set of empirical stellar spectra.

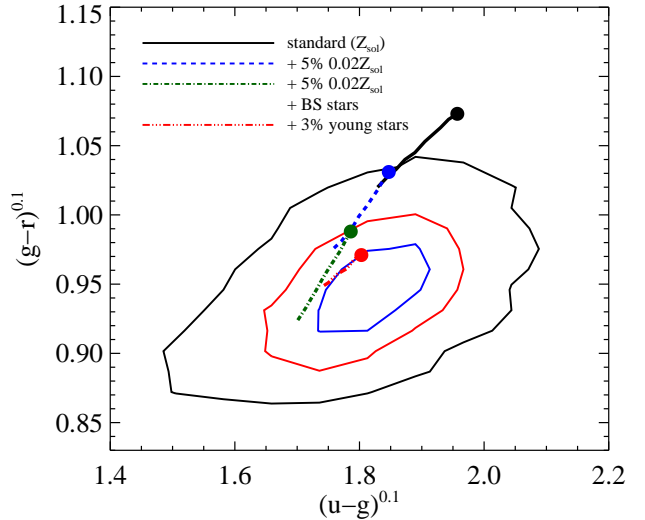


FIG. 15.— Comparison of the observed ugr colors of luminous red sequence galaxies (contours) to FSPS models. All models are dust-free SSPs at $Z = Z_\odot$ for $5 < t < 13$ Gyr, with symbols marking the location of $t = 13$ Gyr. The standard model is compared to models where metal-poor stars, BS stars (with $S_{BS} = 2$), and young stars with an age of 1.0 Gyr, are added on top of the standard model in the proportions noted in the legend.

Indeed, in Figure 13 there are almost no differences between the two isochrone sets for those indices that are measured at $\lambda \lesssim 5000 \text{ \AA}$. The only index that shows appreciable differences is TiO_2 , which is measured at $\lambda \approx 6230 \text{ \AA}$, where the RGB contributes more to the integrated flux than the main sequence turnoff point.

The BC03 and FSPS models compare favorably for the D_n4000 , $[\text{MgFe}]'$, G4300, and TiO_2 indices (except for the $Z = 1.5Z_\odot$ models for the latter index). The $Z = 1.5Z_\odot$ FSPS model predictions for C4668 compare more favorably with the data than the BC03 model of comparable metallicity, while the converse is true for the Fe4531 index. The differences between the BC03 and FSPS models are most dramatic in the $H\delta_A - D_n4000$ plane, where the BC03 $H\delta_A$ EWs are larger than the FSPS predictions by $\approx 1.3 \text{ \AA}$, and are in significant discord with the data. This discrepancy has been noted previously by Wild et al. (2007), and is most likely due to deficiencies in the STELIB empirical stellar library used by BC03.

One of the most striking results of these comparisons is that all models tend to over-predict the D_n4000 strength and under-predict the $H\delta_A$ strength, especially for $Z = 1.5Z_\odot$. As can be gleaned from the symbols in the upper left panel of Figure 12, at $Z = 1.5Z_\odot$ the models reproduce the observed D_n4000 locus of massive galaxies for ages 3–6 Gyr, while for $Z = Z_\odot$ the observations are reproduced for somewhat older ages of 6–10 Gyr. From a detailed analysis utilizing multiple spectral indices, Thomas et al. (2005) find most massive ellipticals to have solar to super-solar metallicities and ages > 10 Gyr (see also, e.g., Bower et al. 1992; Bender et al. 1996; Ziegler et al. 1999; Graves & Schiavon 2008). In light of these results, an explanation is required for the discrepancy between observed and predicted D_n4000 and $H\delta_A$ values. Possible explanations are discussed in the following section.

Before considering possible explanations we point out that the proper inclusion of α -enhancement will only exacerbate

the discrepancy between models and data in regards to the $H\delta_A$ index. This occurs because α -enhancement will result in an even weaker $H\delta_A$ index (Prochaska et al. 2007).

4.5. Resolving the model–data discrepancies for quiescent galaxies

In the previous section two striking disagreements were noted between SPS models and a sample of massive red sequence galaxies. Assuming that such galaxies are composed of ‘normal’ stars¹² of at least solar metallicity and with ages > 10 Gyr, all SPS models predict ugr colors that are too red, D_n4000 strengths that are too large, and $H\delta_A$ strengths that are too weak.

There are two possible classes of solutions to this discrepancy. In the first class, an appeal is made to deficiencies in either the stellar atmospheres or stellar evolution calculations. Within this class, an appeal to stellar evolution means considering inadequacies in standard phases such as the main sequence and its turn–off point, and the RGB. Solutions of the second class abandon one or more of the assumptions regarding the composition of such galaxies. In this second class appeals are made to minority populations of either young stars or metal–poor stars, or exotic aspects of stellar evolution including blue stragglers and mass-loss leading to an extended horizontal branch. These classes are conceptually different in that the former appeals to a modification of the bulk metal–rich old population while the latter appeals to additions of minority populations. We consider both of these classes below.

4.5.1. Problems with stellar atmospheres and stellar evolution

We find that the discrepancies are unlikely to be due to the stellar spectral libraries. We have considered both the theoretical BaSeL library and the empirical Miles library and find similar disagreements in the colors. The empirical STELIB library used in BC03 yields similar disagreements between both the $g-r$ color and the D_n4000 strengths, further suggesting that the libraries are not at fault.

These results are at odds with Maraston et al. (2009) who showed that the optical spectra and $g-r$ colors of SSPs at Z_\odot are markedly different when comparing models constructed using the BaSeL spectral library and the empirical Pickles (1998) library. The purported discrepancies caused by the spectral libraries cannot be reproduced with our FSPS code when using the empirical Miles library. To test that this was not due to differences between the Miles and Pickles library, we also compared spectra generated from the BC03 model using both the BaSeL and Pickles library and again find no substantial difference in $g-r$ colors. We have also compared the spectra of individual stars from the Pickles, Miles, and BaSeL libraries for the same stellar parameters discussed by Maraston et al. and again cannot reproduce their results (i.e., their Figure 4).

We also point out that in the context of the explanation proposed by Maraston et al., the BaSeL library should provide a better fit to the data when the colors are k -corrected to $z = 0.0$ (as opposed to $z = 0.1$), because their discrepancy arises in a region of the spectrum sampled by the r -band redshifted to $z = 0.1$. However, when we compare the colors of $z \lesssim 0.03$ red sequence galaxies we find that the model discrepancies remain.

¹² ‘Normal’ here is meant to exclude such stellar phases as blue stragglers and hot horizontal branch stars.

The discrepancy is also unlikely to be due to unresolved issues with canonical phases of stellar evolution such as the main sequence and RGB, because the aspects of stellar evolution relevant for ugr colors are adequately described by the models for old, metal–rich star clusters. This claim is based on two observations. First, from Figure 7 it is clear that FSPS can reproduce the main sequence turn–off point and base of the RGB of old, metal–rich star clusters. This is especially the case for UBV colors of the clusters NGC 6791 and NGC 188. To the extent that there are residual discrepancies, the models tend to be somewhat too blue compared to the data, which is in the opposite sense of the discrepancies noted for galaxies. Second, in Figure 8 it was shown that for blue colors such as $B-V$, one need not probe the brightest portions of the RGB in order to achieve convergence in the integrated color (the results for $g-r$ are very similar to $B-V$). Therefore, integrated $g-r$ colors of old metal–rich clusters should be accurate because the main sequence turn–off and the base of the RGB are relatively well–fit by the model in the CMD.

In sum, we believe that the discrepancies between model and data ugr colors and spectral indices are not a reflection of the limitations of either stellar atmospheres or canonical aspects of stellar evolution.

4.5.2. Minority populations in predominantly old metal–rich galaxies

There are two remaining possible solutions to the disagreement between models and data for massive red sequence galaxies, which we lump into one class because they share the common property of being minority additions to the dominant, old metal–rich population. The first solution consists of modifications to the SSPs. This solution includes the addition of BS or blue HB stars.

The second solution to these disagreements lies not in trying to fix the SSPs but rather in relaxing the implicit assumption that these massive red galaxies are composed of mono–metallic, coeval stars. Indeed, estimates of the metallicities of stars in our own and nearby galaxies, either from direct spectroscopy or via the colors of giant branch stars, always yield a metallicity distribution function that is approximately lognormal with a full width of ≈ 1 dex (Rich 1990; Grillmair et al. 1996; Harris et al. 1999; Zoccali et al. 2003; Worthey et al. 2005; Sarajedini & Jablonka 2005; Koch et al. 2006). Models for the chemical evolution of galaxies also generically predict that galaxies should contain stars of a range of metallicities, including a non–trivial fraction of metal–poor stars (Searle & Sargent 1972; Pagel 1997).

Extreme/blue HBs exist in the solar and super–solar metallicity star clusters NGC 188 (Landsman et al. 1998) and NGC 6791 (Landsman et al. 1998; Kalirai et al. 2007), in addition to moderately sub–solar clusters (Rich et al. 1997). Resolved UV photometry in the nucleus of M32 has shown that $\sim 5\%$ of HB stars are hot (Brown et al. 2000). Moreover, many metal–rich clusters contain copious BS populations (e.g., Landsman et al. 1998; Zoccali et al. 2001; Kalirai et al. 2007). These observations suggest that it would be prudent to consider models that allow for blue/extended HBs and BS stars to be associated with metal–rich populations. In our treatment we are agnostic as to which population (metal–rich or metal–poor) these hot stars are associated with.

These various effects are explored in Figures 14 and 15. In these figures we explore the impact of various modifications to the base dust–free SSP models. Modifications include: 1) a small fraction (1–3%) of young ($t = 1.0$ Gyr) stars; 2) a

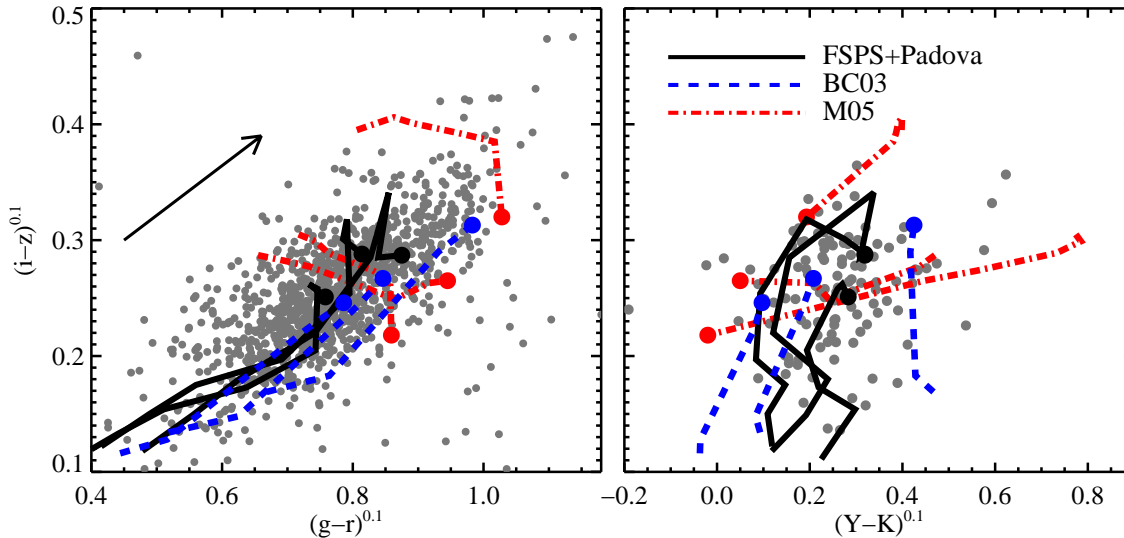


FIG. 16.— Color-color diagrams comparing observed K+A (post-starburst) galaxies (*grey symbols*) to both our FSPS model and the models of BC03 and M05. For BC03 and M05, the colors of SSPs are plotted for ages $0.8 < t < 2.5$ Gyr for three metallicities: $\log(Z/Z_{\odot}) \approx -0.2, 0.0, 0.2$ (corresponding to three lines for each model). FSPS models are shown for a τ -model SFH with $\tau = 0.1$ Gyr, for the same age and metallicity ranges as the other models. The choice of a composite SFH for FSPS was chosen for cosmetic reasons only. Symbols along the model predictions mark $t = 2.5$ Gyr. In the left panel the arrow indicates the change in colors that would occur from adding dust with $A_V = 0.5$ and a Calzetti et al. (1994) reddening curve. As discussed in the text, the addition of an underlying old population moves the models along the reddening vector, which is also along the locus of observed *griz* colors.

population of blue HB stars ($f_{\text{BHB}} = 0.2$); 3) a population of BS stars ($S_{\text{BS}} = 2$); 4) a minority population (5%) of metal-poor stars.

All of these modifications move the base SSP models in the correct qualitative sense; that is they result in lower values of D_n4000 and larger $H\delta_A$ strengths, and bluer *ugr* colors. These trends result from the fact that each modification is adding a population of relatively hot stars, whether in the form of a hotter main sequence turnoff (as happens when metal-poor stars are added), hot evolved stars including BS and blue HB stars, or hot young stars. Hotter stars have lower values of D_n4000 , larger balmer absorption, and bluer continua.

4.5.3. Summary and outlook

The discrepancies discussed above between SSP predictions and massive Elliptical galaxies have been known, in one form or another, for decades (e.g., Faber 1977; Oconnell 1980; Gunn et al. 1981; Rose 1985; Schweizer et al. 1990; Schweizer & Seitzer 1992; Worthey et al. 1996; Maraston & Thomas 2000; Caldwell et al. 2003; Trager et al. 2005; Schiavon 2007). Our contribution to this issue has been twofold: 1) to highlight the connection between the indices and broadband *ugr* colors, in the sense that whatever hot star population is adopted, it should alleviate the discrepancies seen in both indices and colors; 2) to remind the user of SPS models that reliable results concerning the ages and metallicities of massive Ellipticals cannot be attained unless these minority hot star populations are carefully considered.

Many previous studies have considered one or more of the minority populations considered herein as a remedy to the model discrepancies. Schiavon (2007) disfavours appeals to blue HB stars based on the consideration of higher-order balmer lines in Ellipticals. However, this conclusion rests on the assumption that the temperature distribution along the HB in other galaxies is similar to that seen in the MW. While this may seem to be a relatively benign assumption, recent UV

observations of clusters in M87 cast doubt on this (Sohn et al. 2006). If the M87 result holds up to further scrutiny, it will mean that insights from the MW star cluster population cannot be readily applied to other galaxies. This would be a dramatic setback to our attempts at understanding the stellar populations in other galaxies, and would have potentially profound implications for our understanding of stellar evolution.

The addition of metal-poor stars is rarely considered without also considering the addition of blue HB stars. In this work we have separated these two populations, since the observed relation between metallicity and HB morphology in the MW is complex and displays considerable scatter (Piotto et al. 2002). It should be remembered that in every galaxy where metallicity distribution functions have been measured, there exist metal-poor stars ($\log(Z/Z_{\odot}) \lesssim -1$) in sufficient numbers ($\approx 1-5\%$; e.g., Harris et al. 1999; Zoccali et al. 2003; Sarajedini & Jablonka 2005) to effect the integrated blue/UV flux. Given this observational fact, metal-poor stars *must* be included in the models; the only question that remains is in what proportion.

It is something of a disappointment that the identification of the hot star population in Ellipticals remains unresolved more than three decades after it was first discussed. Despite enormous advances in both the SPS models and the quality of the data, the fundamental problem remains that these various hot star populations occupy essentially the same (or similar) ranges in T_{eff} . We briefly comment on several possible future directions that might help separate the relative influence of these various populations.

If young stars or metal-poor stars are the dominant contributor, then because their metallicities will differ from the bulk population, metallicities measured in the blue/UV will differ from metallicities measured in the red. Models will have to be constructed to determine whether or not this effect is measurable. If it is then this could be a promising means of

discriminating between the various hot star candidates.

If young stars are the culprit, then lookback studies of Ellipticals will uncover Ellipticals with younger and younger minority populations. Such a study would suffer from the typical difficulties in lookback studies, namely that precise descendant–progenitor relations are difficult to construct. However, with new and upcoming wide–field spectroscopic surveys we believe that the difficulties associated with lookback studies can be mitigated. Lookback studies might also be able isolate the importance of blue HB stars (Atlee et al. 2009).

A final, somewhat more speculative possibility, is the use of SBFs in the blue to discriminate between these various populations. While these populations occupy approximately the same range of T_{eff} , they all occupy rather different ranges in L_{bol} , and they will thus produce different SBF magnitudes in the blue. We are currently constructing models aimed at determining whether or not such an effect is observable with current facilities.

4.6. Constraints from post–starburst galaxies

K+A, or post–starburst, galaxies offer a unique constraint on intermediate age populations. The prominent A star spectra in these galaxies without any accompanying H α emission (i.e., no *current* star formation), indicates that they are dominated by stars with ages ≈ 1 –2 Gyr. Such galaxies can therefore provide potentially strong constraints on the importance of TP–AGB stars, since such stars peak in prominence at ages ≈ 1 –2 Gyr.

Figure 16 compares the colors of K+A galaxies defined by Quintero et al. (2004) to the colors of dust–free SSPs at ages $0.8 < t < 2.5$ Gyr for metallicities $\log(Z/Z_{\odot}) \approx -0.2, 0.0, 0.2$. Model predictions from FSPS (using the Padova isochrones), M05, and BC03 are shown. The FSPS model predictions are shown for a τ –model SFH ($\text{SFR} \propto e^{-t/\tau}$) with $\tau = 0.1$ Gyr for cosmetic reasons only. Recall that the TP–AGB phase in the Padova isochrones was modified in order to produce acceptable agreement with both the MC star clusters and these post–starburst galaxies (although the modifications are slight for intermediate ages at solar metallicity; see §3.1.3). While not shown, FSPS predictions using the BaSTI isochrones are similar to the Padova isochrones. A reddening vector is shown to indicate the shift in colors expected for a uniform screen of dust with optical depth $A_V = 0.5$ and a Calzetti et al. (1994) attenuation law.

The ratio of A to K stars in the observed spectra decreases with increasing $g-r$ and $i-z$ colors, indicating that the sequence in the left panel is primarily a sequence in age, and not dust nor metallicity. This observational fact will be a significant discriminator amongst the SPS models considered herein.

The FSPS model predictions encompass the range of observed $i-z$, $g-r$, and $Y-K$ colors. The dominant variable driving the change in model colors is age, in agreement with the data. The BC03 model predictions are somewhat too blue in $i-z$, although we believe that the agreement is acceptable given the fact that post–starburst galaxies are composite populations whereas we have modeled them as single populations (see below).

In contrast to the FSPS and BC03 models, the M05 model performs poorly in $g-r$ and $i-z$ colors. In particular, model sequences of increasing age produce trends in these colors that are orthogonal to the observed trends with age. In the context of the M05 model the increasing $g-r$ and $i-z$ colors

would be interpreted as a sequence of either increasing dust content or increasing metallicity. This interpretation would be in contrast with the observed variation in the spectral properties. It is also difficult to explain the bluer half of the observed K+A galaxies in $griz$ colors unless unrealistically low metallicities are considered. Appealing to younger ages does not remedy this either, as M05 model predictions at younger ages ($t < 0.8$ Gyr) continues to diverge from the locus of observed colors.

As discussed in previous sections, it is difficult to reliably calibrate SPS models against galaxies because galaxies contain stars of a range of metallicities and ages, and the effects of dust cannot be ignored. Here we have been considering a dust–free, mono–metallic, coeval population model. For the comparisons in this section, these complications turn out to have minimal consequences regarding the model comparisons. For example, as shown in Figure 16, the dust reddening vector lies parallel to the locus of data, and so dust effects cannot move the models onto or off of the observed locus, but only along the locus. Since our conclusions do not rely on the detailed location of the models along the observed locus, our results are insensitive to dust effects.

We have also considered the effects of adding an old population on top of the intermediate age, post–starburst population. Even in the extreme case where 90% of the mass is contained in an old population and only 10% spans the intermediate age range of $0.8 < t < 2.5$ Gyr, the red end of the model predictions only shift slightly toward redder colors. The primary effect of an addition of an old population is a narrowing of the range in color of the model predictions. In any event, the addition of old stars has an effect similar to dust attenuation — namely, the models shift along the observed locus. We conclude that, in the case of post–starburst galaxies and for the colors we have considered, composite population effects do not impact our conclusions.

5. MODEL EVALUATION

In the previous section we explored the constraints on several SPS models provided by star cluster data in the Local Group and M87 and by post–starburst and massive red sequence galaxies. We now summarize these results and provide a general evaluation of the models.

Star clusters in the MCs provide valuable constraints on models at intermediate age and sub–solar metallicities. The M05 model performs poorly when compared to the extant data, while the BC03 model performs better, although the BC03 model is somewhat too blue in the near–IR. In M05, the colors are too red and the age–dependence is incorrect. The incorrect age–dependence in M05 cannot be attributed to the details of MC cluster age estimation. Our own FSPS model with Padova isochrones is able to achieve excellent agreement with the data only after we modify the TP–AGB phase of the input Padova isochrones. The BaSTI isochrones in FSPS fare well, although less–so in the near–IR, which plausibly reflects their simplistic TP–AGB treatment, and, at young ages, which may be due to our use of the BaSTI isochrones that suppresses convective overshooting. Similar conclusions are reached regarding the FSPS model when considering constraints afforded by SBFs of MC star clusters.

The MW and M31 provide a large sample of old, metal–poor star clusters, but only a small handful of old metal–rich clusters. The FSPS (using both the Padova and BaSTI isochrones), BC03, and M05 models all make similar predictions for the $UBVR IJHK$ photometry of old metal–poor sys-

tems. The models compare favorably in *UBVRI* colors once uncertainties in the filter transmission curves are considered.

In the near-IR the models perform less well, where for example *V-K* colors are too blue by ≈ 0.2 mags at $\log(Z/Z_{\odot}) > -1.0$. The origin of this discrepancy is unclear, but may either be due to an RGB that is too hot (lowering the RGB by 200K would alleviate this tension) or stellar libraries that are inadequate in the near-IR. At higher metallicity, multi-color CMDs in *UBVIK* colors are well reproduced by the FSPS model in regards to the location of the turn-off point, sub-giant branch, and the lower portion of the RGB. We demonstrate that agreement in CMD-space between data and models does not imply that the integrated colors are adequately constrained because the integrated colors in the red and near-IR are dominated by the brightest stars in the cluster. These stars are rarely included in CMD studies because they are rare and often saturate the photometry. In any event, even if these stars are considered, owing to their rarity it is challenging to reliably calibrate models in this regime in CMD-space. It is for this reason that we focus our calibrations on integrated cluster properties, rather than resolved CMDs.

The spectral indices D_n4000 and $H\delta_A$ of MW star clusters are not adequately reproduced by either the FSPS or BC03 model at high and low metallicities, respectively (the M05 model does not contain sufficient spectral resolution to make a robust prediction). These inadequacies are removed if BS or hot HB stars are added.

In the ultraviolet, the FSPS model can reproduce the observed trends because the relevant phases — post-AGB and HB — are handled flexibly and so can be tuned to match the data. The BC03 and M05 models generally fare less well, either because of the omission of blue HB stars (BC03) or post-AGB stars (M05).

Turning to galaxies, all models predict *ugr* colors of red sequence galaxies that are too red and the FSPS and BC03 models predict D_n4000 strengths that are too strong (again, the M05 model does not contain the requisite resolution), under the assumption that such galaxies are composed solely of old stars with $Z \geq Z_{\odot}$. These issues are likely closely connected to the model failures at reproducing the spectral features of metal-rich MW star clusters. These discrepancies can be removed by adding a minority population of hot stars, coming either from metal-poor turn-off stars, hot HB stars, BS stars, or young (~ 1 Gyr) stars.

The FSPS and BC03 models are able to reproduce the optical and near-IR colors of post-starburst galaxies, while the M05 model performs less well. These galaxies likely have a preponderance of TP-AGB stars, and so they provide valuable constraints on this phase.

In summary, our FSPS model is able to reproduce the greatest range of observations, due in large part to the flexibility of the model. BC03 fares somewhat less well, and M05 performs worst of the three. Even where calibrating data is available, significant discrepancies remain. Important regions of parameter space do not contain sufficient calibrating data, and so the models are even less reliable there. Finally, when modeling predominantly old, metal-rich populations, care must be taken to include minority populations of hot stars.

5.1. Comments on other SPS models

In this section we comment on a number of other SPS models in the literature. The main purpose of the following discussion is to highlight the fact that many SPS models rely on the same ingredients as the models considered in detail herein,

and therefore conclusions reached in earlier sections should be applicable to other models as well.

The most popular SPS models not considered herein are Starburst99 (Leitherer et al. 1999; Vázquez & Leitherer 2005) and Pegase (Fioc & Rocca-Volmerange 1997; Le Borgne et al. 2004). In its most current version, Starburst99 combines the Geneva models for massive stars and the Padova isochrones for intermediate and low mass stars. Starburst99 employs the TP-AGB models of Vassiliadis & Wood (1993), which are the same models used in BC03. The BaSeL stellar library is used to convert the models into observable SEDs. For hot stars, the theoretical models of Smith et al. (2002) are used.

For stellar populations not dominated by massive stars, Starburst99 will produce results similar to BC03. The treatment of nebular emission and massive stars, including Wolf-Rayet stars, is more sophisticated than either FSPS, M05, or BC03, and should therefore continue to be the model of choice when emission from massive stars is important. The recent Popstar model (Mollá et al. 2009) also contains a sophisticated treatment of massive stars, including the theoretical atmosphere models for O and Wolf-Rayet stars of Smith et al. (2002), and will therefore produce results similar to Starburst99.

Pegase utilizes the Padova isochrones and couples these to two different stellar spectral libraries: BaSeL, and ELODIE (Prugniel & Soubiran 2001). ELODIE is an empirical library of ≈ 1500 stars. In Le Borgne et al. (2004), various spectral indices are computed with Pegase and compared to observations. The comparisons focus on a small sample of indices (including $H\beta$, Fe5270, Mgb, and Fe5335) for Elliptical galaxies and MW star clusters. It would be fruitful to consider more comprehensive calibrating comparisons for the Pegase model, such as is considered herein. In any event, the underlying isochrones are similar to those used in BC03, so the predictions of Pegase should be similar to BC03.

The Vazdekis models are described in Vazdekis (1999), Vazdekis et al. (2003), and Vazdekis et al. (in prep). They utilize the Padova isochrones coupled to the empirical Miles stellar library. For old populations this model should thus be essentially identical to the FSPS predictions when the unmodified Padova isochrones are used. The Vazdekis model may thus fail to reproduce the observed near-IR colors of MC star clusters, since, as we demonstrated, the unmodified Padova isochrones are a poor match to those data.

Significant efforts are currently underway to generate SPS models that handle α -enhancement self-consistently, in the sense that both the stellar evolution calculations and the atmosphere models have the same abundance patterns (e.g., Coelho et al. 2007; Lee et al. 2009c). These models will provide valuable constraints on the relative effects of α -enhancement. However, most models currently only follow stellar evolution through the end of the RGB, and so they cannot be used on their own to build model galaxies (the exception to this is the BaSTI database; Cordier et al. 2007; Percival et al. 2009). We anticipate that the treatment of α -enhancement as a variable on par with age and Z in SPS models will likely become commonplace in the near future.

From the above discussion it should be clear that the majority of SPS codes use the Padova isochrones with the BaSeL stellar library. Our comparisons and evaluations in previous sections, which rely on these ingredients, should therefore be applicable to many other SPS models.

6. SUMMARY

We now summarize our principle results.

- The latest stellar models from the Padova group cannot fit the near-IR photometry and surface brightness fluctuations of star clusters in the MCs. With our flexible SPS (FSPS) code we have modified the TP-AGB phase in the Padova isochrones to produce better fits to the data. The M05 models also fail to reproduce the data, both because the colors are too red and the age-dependence is incorrect. The BC03 and the FSPS model using the BaSTI isochrones fare well, although both models are somewhat too blue in the near-IR. A significant limiting factor in more accurate calibrations is the difficulty in constructing reliable photometry of MC clusters, owing to the fact that TP-AGB stars are luminous and rare.
 - At low metallicities ($\log(Z/Z_{\odot}) < -0.5$) and old ages, all models predict similar $UBVRIZJK$ colors (the typical variation between models is ≈ 0.05 mags). When compared to MW and M31 star clusters, the models are 0.2 mags too blue in $V-K$ at $\log(Z/Z_{\odot}) > -1.0$, and 0.1 mags too red in $J-K$ at all Z . The origin of the discrepancies in the near-IR is unclear. Decreasing the temperature of the RGB by $\sim 200\text{K}$ alleviates much of the disagreement. If this modification is isolated to the brightest stars, then such a modification could improve agreement with integrated photometry without compromising agreement in CMD-space. The FSPS model with the BaSTI isochrones performs worst at low metallicities and old ages of the models considered (although the disagreement is not dramatic), while the FSPS model with the Padova isochrones performs well.
- Multi-color CMDs of two metal-rich clusters, NGC 6791 and NGC 188, are well-fit by FSPS. Spectral indices of MW star clusters are generally well-fit by both FSPS and BC03, although the models predict D_n4000 strengths too large and $H\delta_A$ strengths too weak compared to two $\log(Z/Z_{\odot}) \approx 0.0$ clusters.
- The ultraviolet photometry of the MW, M87, and M31 star clusters can be well-fit by FSPS because FSPS contains flexible treatments of the post-AGB and horizontal branch evolutionary phases. This flexibility is essential given the substantial scatter in the ultraviolet data at fixed metallicity, and given our inadequate theoretical understanding of these phases. The M05 and BC03 models perform less well because of their incomplete treatment of these advanced evolutionary phases.
 - SPS models are compared to $ugrzYJHK$ photometry of massive red sequence galaxies. The FSPS, BC03, and M05 models fare well in most respects, with a few exceptions: all models are too blue in $J-H$; the M05 model is somewhat too blue in $Y-K$; all models are far too red in $g-r$ and $u-g$. These conclusions hold under the assumption that red sequence galaxies are com-

posed exclusively of old metal-rich stars with canonical evolutionary phases. The disagreement in the ugr colors can be alleviated if some combination of young (~ 1 Gyr) stars, metal-poor stars, and blue straggler stars are added in small amounts.

- Optical spectral indices of massive galaxies are generally well-fit by the FSPS and BC03 models, with the important exceptions that both models predict D_n4000 in excess of observations and neither fit the observed locus of galaxies in the $D_n4000-H\delta_A$ plane. These conclusions hold for the same assumptions noted above, and, as above, small additions of some combination of young stars, metal-poor stars, blue straggler and horizontal branch stars can remedy this disagreement.
- The FSPS and BC03 models adequately describe the $grizYK$ colors of K+A, or ‘post-starburst’ galaxies, while the M05 model performs less well. Such galaxies contain a large proportion of intermediate age ($0.5 < t < 2$ Gyr) stars and thus provide unique constraints on the importance of TP-AGB stars in galaxies.

We thank David Hogg for providing the K+A galaxy catalog, Patricia Sánchez-Blázquez for providing the Miles library in electronic format, Rita Gautschy for providing her model results, the BaSTI, Padova, BaSeL, and MPA/JHU groups for publically releasing their results and for assistance in their use, and Tony Sohn for help with interpretation of the ultraviolet star cluster data. Santi Cassisi, David Hogg, Claudia Maraston and Ricardo Schiavon are thanked for comments on an earlier draft.

Funding for the Sloan Digital Sky Survey (SDSS) has been provided by the Alfred P. Sloan Foundation, the Participating Institutions, the National Aeronautics and Space Administration, the National Science Foundation, the U.S. Department of Energy, the Japanese Monbukagakusho, and the Max Planck Society. The SDSS Web site is <http://www.sdss.org/>.

The SDSS is managed by the Astrophysical Research Consortium (ARC) for the Participating Institutions. The Participating Institutions are The University of Chicago, Fermilab, the Institute for Advanced Study, the Japan Participation Group, The Johns Hopkins University, Los Alamos National Laboratory, the Max-Planck-Institute for Astronomy (MPIA), the Max-Planck-Institute for Astrophysics (MPA), New Mexico State University, University of Pittsburgh, Princeton University, the United States Naval Observatory, and the University of Washington.

This publication makes use of data products from the Two Micron All Sky Survey, which is a joint project of the University of Massachusetts and the Infrared Processing and Analysis Center/California Institute of Technology, funded by the National Aeronautics and Space Administration and the National Science Foundation.

This work made extensive use of the NASA Astrophysics Data System and of the `astro-ph` preprint archive at [arXiv.org](http://arxiv.org).

REFERENCES

- Allard, F. & Hauschildt, P. H. 1995, *ApJ*, 445, 433
 Alongi, M., Bertelli, G., Bressan, A., Chiosi, C., Fagotto, F., Greggio, L., & Nasi, E. 1993, *A&AS*, 97, 851
 An, D. et al. 2009, *ApJ*, 700, 523
 Atlee, D. W., Assef, R. J., & Kochanek, C. S. 2009, *ApJ*, 694, 1539

- Barmby, P., Huchra, J. P., Brodie, J. P., Forbes, D. A., Schroder, L. L., & Grillmair, C. J. 2000, *AJ*, 119, 727
- Bender, R., Ziegler, B., & Bruzual, G. 1996, *ApJ*, 463, L51
- Bessell, M. S., Brett, J. M., Scholz, M., & Wood, P. R. 1991, *A&AS*, 89, 335
- Bessell, M. S., Brett, J. M., Wood, P. R., & Scholz, M. 1989, *A&AS*, 77, 1
- Blanton, M. R. & Roweis, S. 2007, *AJ*, 133, 734
- Blanton, M. R. et al. 2005, *AJ*, 129, 2562
- Bower, R. G., Lucey, J. R., & Ellis, R. S. 1992, *MNRAS*, 254, 601
- Bressan, A., Fagotto, F., Bertelli, G., & Chiosi, C. 1993, *A&AS*, 100, 647
- Brown, T. M., Bowers, C. W., Kimble, R. A., Sweigart, A. V., & Ferguson, H. C. 2000, *ApJ*, 532, 308
- Brown, T. M., Smith, E., Ferguson, H. C., Sweigart, A. V., Kimble, R. A., & Bowers, C. W. 2008, *ApJ*, 682, 319
- Bruzual, G. 1983, *ApJ*, 273, 105
- Bruzual, G. & Charlot, S. 1993, *ApJ*, 405, 538
- . 2003, *MNRAS*, 344, 1000
- Bruzual A., G. 2002, in *IAU Symposium*, Vol. 207, *Extragalactic Star Clusters*, ed. D. P. Geisler, E. K. Grebel, & D. Minniti, 616
- Burstein, D., Bertola, F., Buson, L. M., Faber, S. M., & Lauer, T. R. 1988, *ApJ*, 328, 440
- Buzzoni, A. 1989, *ApJS*, 71, 817
- Caldwell, N., Rose, J. A., & Concannon, K. D. 2003, *AJ*, 125, 2891
- Calzetti, D., Kinney, A. L., & Storchi-Bergmann, T. 1994, *ApJ*, 429, 582
- Cardelli, J. A., Clayton, G. C., & Mathis, J. S. 1989, *ApJ*, 345, 245
- Carney, B. W., Lee, J., & Dodson, B. 2005, *AJ*, 129, 656
- Carpenter, J. M. 2001, *AJ*, 121, 2851
- Carretta, E., Bragaglia, A., Gratton, R., D'Orazi, V., & Lucatello, S. 2009, *ArXiv:0910.0675*
- Carter, D. et al. 2009, *MNRAS*, 397, 695
- Casali, M. et al. 2007, *A&A*, 467, 777
- Cassisi, S. 2007, in *IAU Symposium*, Vol. 241, *IAU Symposium*, ed. A. Vazdekis & R. F. Peletier, 3–12
- Cassisi, S., Castellani, V., Ciarcelluti, P., Piotto, G., & Zoccali, M. 2000, *MNRAS*, 315, 679
- Cassisi, S., degl'Innocenti, S., & Salaris, M. 1997, *MNRAS*, 290, 515
- Catelan, M. 2009, *Ap&SS*, 320, 261
- Cenarro, A. J. et al. 2007, *MNRAS*, 374, 664
- Cerviño, M. & Luridiana, V. 2004, *A&A*, 413, 145
- Charlot, S. 1996, in *Astronomical Society of the Pacific Conference Series*, Vol. 98, *From Stars to Galaxies: the Impact of Stellar Physics on Galaxy Evolution*, 275
- Charlot, S., Worthey, G., & Bressan, A. 1996, *ApJ*, 457, 625
- Coelho, P., Bruzual, G., Charlot, S., Weiss, A., Barbuy, B., & Ferguson, J. W. 2007, *MNRAS*, 382, 498
- Cohen, J. G. 1982, *ApJ*, 258, 143
- Cohen, J. G., Hsieh, S., Metchev, S., Djorgovski, S. G., & Malkan, M. 2007, *AJ*, 133, 99
- Conroy, C., Gunn, J. E., & White, M. 2009a, *ApJ*, 699, 486
- Conroy, C., White, M., & Gunn, J. E. 2009b, *ArXiv:0904.0002*
- Cordier, D., Pietrinfermi, A., Cassisi, S., & Salaris, M. 2007, *AJ*, 133, 468
- Dorman, B., O'Connell, R. W., & Rood, R. T. 1995, *ApJ*, 442, 105
- Dressler, A. & Gunn, J. E. 1983, *ApJ*, 270, 7
- Eldridge, J. J., Izzard, R. G., & Tout, C. A. 2008, *MNRAS*, 384, 1109
- Elson, R. A. W. & Fall, S. M. 1985, *ApJ*, 299, 211
- Eminian, C., Kauffmann, G., Charlot, S., Wild, V., Bruzual, G., Rettura, A., & Loveday, J. 2008, *MNRAS*, 384, 930
- Epchtein, N. et al. 1997, *The Messenger*, 87, 27
- Faber, S. M. 1977, in *Evolution of Galaxies and Stellar Populations*, ed. B. M. Tinsley & R. B. Larson, 157
- Fagotto, F., Bressan, A., Bertelli, G., & Chiosi, C. 1994, *A&AS*, 104, 365
- Fioc, M. & Rocca-Volmerange, B. 1997, *A&A*, 326, 950
- Fluks, M. A., Plez, B., The, P. S., de Winter, D., Westerlund, B. E., & Steenman, H. C. 1994, *A&AS*, 105, 311
- Fusi Pecci, F., Bellazzini, M., Buzzoni, A., De Simone, E., Federici, L., & Galletti, S. 2005, *AJ*, 130, 554
- Gallart, C., Zoccali, M., & Aparicio, A. 2005, *ARA&A*, 43, 387
- Galletti, S., Federici, L., Bellazzini, M., Fusi Pecci, F., & Macrina, S. 2004, *A&A*, 416, 917
- Girardi, L., Bressan, A., Bertelli, G., & Chiosi, C. 2000, *A&AS*, 141, 371
- Girardi, L., Chiosi, C., Bertelli, G., & Bressan, A. 1995, *A&A*, 298, 87
- González, R. A., Liu, M. C., & Bruzual A., G. 2004, *ApJ*, 611, 270
- González-Lópezlira, R. A., Albarrán, M. Y., Mouhcine, M., Liu, M. C., Bruzual-A., G., & de Batz, B. 2005, *MNRAS*, 363, 1279
- Goto, T. et al. 2003, *PASJ*, 55, 771
- Graves, G. J. & Schiavon, R. P. 2008, *ApJS*, 177, 446
- Greggio, L. & Renzini, A. 1990, *ApJ*, 364, 35
- Grillmair, C. J. et al. 1996, *AJ*, 112, 1975
- Groenewegen, M. A. T. 2006, *A&A*, 448, 181
- Groenewegen, M. A. T. & de Jong, T. 1993, *A&A*, 267, 410
- Gullieuszik, M., Held, E. V., Rizzi, L., Girardi, L., Marigo, P., & Momany, Y. 2008, *MNRAS*, 388, 1185
- Gunn, J. E., Stryker, L. L., & Tinsley, B. M. 1981, *ApJ*, 249, 48
- Hambly, N. C. et al. 2008, *MNRAS*, 384, 637
- Han, Z., Podsiadlowski, P., & Lynas-Gray, A. E. 2007, *MNRAS*, 380, 1098
- Harris, G. L. H., Harris, W. E., & Poole, G. B. 1999, *AJ*, 117, 855
- Harris, W. E. 1996, *AJ*, 112, 1487
- Hewett, P. C., Warren, S. J., Leggett, S. K., & Hodgkin, S. T. 2006, *MNRAS*, 367, 454
- Hodgkin, S. T., Irwin, M. J., Hewett, P. C., & Warren, S. J. 2009, *MNRAS*, 394, 675
- Höfner, S., Loidl, R., Aringer, B., Jørgensen, U. G., & Hron, J. 2000, in *ESA Special Publication*, Vol. 456, *ISO Beyond the Peaks: The 2nd ISO Workshop on Analytical Spectroscopy*, ed. A. Salama, M. F. Kessler, K. Leech, & B. Schulz, 299
- Jensen, J. B. et al. 2003, *ApJ*, 583, 712
- Jeong, H. et al. 2009, *MNRAS*, 398, 2028
- Jimenez, R., MacDonald, J., Dunlop, J. S., Padoan, P., & Peacock, J. A. 2004, *MNRAS*, 349, 240
- Kalirai, J. S. et al. 2007, *ApJ*, 671, 748
- Kauffmann, G. et al. 2003, *MNRAS*, 341, 33
- Kaviraj, S., Sohn, S. T., O'Connell, R. W., Yoon, S.-J., Lee, Y. W., & Yi, S. K. 2007, *MNRAS*, 377, 987
- Kerber, L. O., Santiago, B. X., & Brocato, E. 2007, *A&A*, 462, 139
- Koch, A. et al. 2006, *AJ*, 131, 895
- Koleva, M., Prugniel, P., Ocvirk, P., Le Borgne, D., & Soubiran, C. 2008, *MNRAS*, 385, 1998
- Kotulla, R., Fritze, U., Weibacher, P., & Anders, P. 2009, *MNRAS*, 396, 462
- Kroupa, P. 2001, *MNRAS*, 322, 231
- Lançon, A. & Mouhcine, M. 2000, in *Astronomical Society of the Pacific Conference Series*, Vol. 211, *Massive Stellar Clusters*, ed. A. Lançon & C. M. Boily, 34
- Lançon, A. & Mouhcine, M. 2002, *A&A*, 393, 167
- Landsman, W., Bohlin, R. C., Neff, S. G., O'Connell, R. W., Roberts, M. S., Smith, A. M., & Stecher, T. P. 1998, *AJ*, 116, 789
- Lawrence, A. et al. 2007, *MNRAS*, 379, 1599
- Le Borgne, D., Rocca-Volmerange, B., Prugniel, P., Lançon, A., Fioc, M., & Soubiran, C. 2004, *A&A*, 425, 881
- Le Borgne, J.-F., Bruzual, G., Pelló, R., Lançon, A., Rocca-Volmerange, B., Sanahuja, B., Schaerer, D., Soubiran, C., & Vílchez-Gómez, R. 2003, *A&A*, 402, 433
- Lee, H., Worthey, G., & Blakeslee, J. P. 2009a, *ArXiv:0902.1177*
- Lee, H., Worthey, G., & Dotter, A. 2009b, *AJ*, 138, 1442
- Lee, H.-c., Worthey, G., Dotter, A., Chaboyer, B., Jevremović, D., Baron, E., Briley, M. M., Ferguson, J. W., Coelho, P., & Trager, S. C. 2009c, *ApJ*, 694, 902
- Lee, H.-c., Worthey, G., Trager, S. C., & Faber, S. M. 2007, *ApJ*, 664, 215
- Leitherer, C. et al. 1999, *ApJS*, 123, 3
- Lejeune, T., Cuisinier, F., & Buser, R. 1997, *A&AS*, 125, 229
- . 1998, *A&AS*, 130, 65
- Leonardi, A. J. & Rose, J. A. 1996, *AJ*, 111, 182
- Li, Z. & Han, Z. 2008, *ApJ*, 685, 225
- Liu, M. C., Graham, J. R., & Charlot, S. 2002, *ApJ*, 564, 216
- Loidl, R., Lançon, A., & Jørgensen, U. G. 2001, *A&A*, 371, 1065
- Maraston, C. 1998, *MNRAS*, 300, 872
- . 2005, *MNRAS*, 362, 799
- Maraston, C., Daddi, E., Renzini, A., Cimatti, A., Dickinson, M., Papovich, C., Pasquali, A., & Pirzkal, N. 2006, *ApJ*, 652, 85
- Maraston, C., Strömbäck, G., Thomas, D., Wake, D. A., & Nichol, R. C. 2009, *MNRAS*, 394, L107
- Maraston, C. & Thomas, D. 2000, *ApJ*, 541, 126
- Marigo, P. & Girardi, L. 2007, *A&A*, 469, 239
- Marigo, P., Girardi, L., Bressan, A., Groenewegen, M. A. T., Silva, L., & Granato, G. L. 2008, *A&A*, 482, 883
- Martin, D. C. et al. 2005, *ApJ*, 619, L11
- Martins, L. P. & Coelho, P. 2007, *MNRAS*, 381, 1329
- Meynet, G. & Maeder, A. 2000, *A&A*, 361, 101
- Milone, A., Sansom, A. E., & Sánchez-Blázquez, P. 2009, *ArXiv:0909.3291*
- Mollá, M., García-Vargas, M. L., & Bressan, A. 2009, *MNRAS*, 398, 451
- Muzzin, A., Marchesini, D., van Dokkum, P. G., Labbé, I., Kriek, M., & Franx, M. 2009, *ApJ*, 701, 1839
- OConnell, R. W. 1980, *ApJ*, 236, 430
- O'Connell, R. W. 1999, *ARA&A*, 37, 603
- Oke, J. B. & Gunn, J. E. 1983, *ApJ*, 266, 713
- Origlia, L., Valenti, E., Rich, R. M., & Ferraro, F. R. 2006, *ApJ*, 646, 499

- Pagel, B. E. J. 1997, *Nucleosynthesis and Chemical Evolution of Galaxies* (Nucleosynthesis and Chemical Evolution of Galaxies, by Bernard E. J. Pagel, pp. 392. ISBN 0521550610. Cambridge, UK: Cambridge University Press, October 1997.)
- Percival, S. M., Salaris, M., Cassisi, S., & Pietrinferni, A. 2009, *ApJ*, 690, 427
- Perrett, K. M., Bridges, T. J., Hanes, D. A., Irwin, M. J., Brodie, J. P., Carter, D., Huchra, J. P., & Watson, F. G. 2002, *AJ*, 123, 2490
- Persson, S. E., Aaronson, M., Cohen, J. G., Frogel, J. A., & Matthews, K. 1983, *ApJ*, 266, 105
- Pessev, P. M., Goudfrooij, P., Puzia, T. H., & Chandar, R. 2006, *AJ*, 132, 781
—, 2008, *MNRAS*, 385, 1535
- Pickles, A. J. 1998, *PASP*, 110, 863
- Pietrinferni, A., Cassisi, S., Salaris, M., & Castelli, F. 2004, *ApJ*, 612, 168
- Piotto, G. et al. 2002, *A&A*, 391, 945
- Preston, G. W. & Sneden, C. 2000, *AJ*, 120, 1014
- Prochaska, L. C., Rose, J. A., Caldwell, N., Castilho, B. V., Concannon, K., Harding, P., Morrison, H., & Schiavon, R. P. 2007, *AJ*, 134, 321
- Prugniel, P. & Soubiran, C. 2001, *A&A*, 369, 1048
- Quintero, A. D. et al. 2004, *ApJ*, 602, 190
- Renzini, A. & Buzzoni, A. 1986, in *Astrophysics and Space Science Library*, Vol. 122, *Spectral Evolution of Galaxies*, ed. C. Chiosi & A. Renzini, 195–231
- Rey, S.-C. et al. 2007, *ApJS*, 173, 643
- Rich, R. M. 1990, *ApJ*, 362, 604
- Rich, R. M. et al. 1997, *ApJ*, 484, L25
- Rose, J. A. 1985, *AJ*, 90, 1927
- Sánchez-Blázquez, P., Peletier, R. F., Jiménez-Vicente, J., Cardiel, N., Cenarro, A. J., Falcón-Barroso, J., Gorgas, J., Selam, S., & Vazdekis, A. 2006, *MNRAS*, 371, 703
- Sarajedini, A. & Jablonka, P. 2005, *AJ*, 130, 1627
- Sarajedini, A., von Hippel, T., Kozhurina-Platais, V., & Demarque, P. 1999, *AJ*, 118, 2894
- Schiavon, R. P. 2007, *ApJS*, 171, 146
- Schiavon, R. P., Rose, J. A., Courteau, S., & MacArthur, L. A. 2005, *ApJS*, 160, 163
- Schlegel, D. J., Finkbeiner, D. P., & Davis, M. 1998, *ApJ*, 500, 525
- Schweizer, F. & Seitzer, P. 1992, *AJ*, 104, 1039
- Schweizer, F., Seitzer, P., Faber, S. M., Burstein, D., Dalle Ore, C. M., & Gonzalez, J. J. 1990, *ApJ*, 364, L33
- Searle, L. & Sargent, W. L. W. 1972, *ApJ*, 173, 25
- Searle, L., Wilkinson, A., & Bagnuolo, W. G. 1980, *ApJ*, 239, 803
- Skrutskie, M. F. et al. 2006, *AJ*, 131, 1163
- Smith, L. J., Norris, R. P. F., & Crowther, P. A. 2002, *MNRAS*, 337, 1309
- Sohn, S. T., O’Connell, R. W., Kundu, A., Landsman, W. B., Burstein, D., Bohlin, R. C., Frogel, J. A., & Rose, J. A. 2006, *AJ*, 131, 866
- Stetson, P. B., Bruntt, H., & Grundahl, F. 2003, *PASP*, 115, 413
- Thomas, D., Maraston, C., & Bender, R. 2003, *MNRAS*, 339, 897
- Thomas, D., Maraston, C., Bender, R., & Mendes de Oliveira, C. 2005, *ApJ*, 621, 673
- Tinsley, B. M. 1980, *Fundamentals of Cosmic Physics*, 5, 287
- Tinsley, B. M. & Gunn, J. E. 1976, *ApJ*, 203, 52
- Trager, S. C., Faber, S. M., Worthey, G., & González, J. J. 2000, *AJ*, 120, 165
- Trager, S. C., Worthey, G., Faber, S. M., & Dressler, A. 2005, *MNRAS*, 362, 2
- van den Bergh, S. 1981, *A&AS*, 46, 79
- Vassiliadis, E. & Wood, P. R. 1993, *ApJ*, 413, 641
—, 1994, *ApJS*, 92, 125
- Vazdekis, A. 1999, *ApJ*, 513, 224
- Vazdekis, A., Cenarro, A. J., Gorgas, J., Cardiel, N., & Peletier, R. F. 2003, *MNRAS*, 340, 1317
- Vázquez, G. A. & Leitherer, C. 2005, *ApJ*, 621, 695
- Westera, P., Lejeune, T., Buser, R., Cuisinier, F., & Bruzual, G. 2002, *A&A*, 381, 524
- Wild, V., Kauffmann, G., Heckman, T., Charlot, S., Lemson, G., Brinchmann, J., Reichard, T., & Pasquali, A. 2007, *MNRAS*, 381, 543
- Worthey, G. 1994, *ApJS*, 95, 107
- Worthey, G., Dorman, B., & Jones, L. A. 1996, *AJ*, 112, 948
- Worthey, G., España, A., MacArthur, L. A., & Courteau, S. 2005, *ApJ*, 631, 820
- Worthey, G., Faber, S. M., & Gonzalez, J. J. 1992, *ApJ*, 398, 69
- Worthey, G., Faber, S. M., Gonzalez, J. J., & Burstein, D. 1994, *ApJS*, 94, 687
- Xin, Y. & Deng, L. 2005, *ApJ*, 619, 824
- Yi, S. K. 2003, *ApJ*, 582, 202
- Yi, S. K., Kim, Y.-C., & Demarque, P. 2003, *ApJS*, 144, 259
- York, D. G. et al. 2000, *AJ*, 120, 1579
- Ziegler, B. L., Saglia, R. P., Bender, R., Belloni, P., Greggio, L., & Seitz, S. 1999, *A&A*, 346, 13
- Zoccali, M., Renzini, A., Ortolani, S., Bica, E., & Barbu, B. 2001, *AJ*, 121, 2638
- Zoccali, M. et al. 2003, *A&A*, 399, 931